

# ABSTRACTS



## DISTINGUISHED GUEST LECTURES & ORAL PRESENTATIONS

## Acknowledgments

The organizers and delegates of LEEMPEEM6 are very appreciative of the support given by the following institutions as well as the industrial sponsors and exhibitors:

	<p><b>Elettra – Sincrotrone Trieste S.C.p.A</b></p> <p>Elettra is a multidisciplinary Synchrotron Light Laboratory open to researchers in diverse basic and applied fields. The laboratory is equipped with ultra-bright light sources in the spectral range from UV to X-rays and offers a stimulating and competitive environment to researchers from all over the world</p> <p><b>Web:</b> <a href="http://www.elettra.trieste.it">http://www.elettra.trieste.it</a></p>
	<p><b>Integrated Infrastructure Initiative (I3) "Integrating Activity on Synchrotron and Free Electron Laser Science" (IA-SFS)"</b></p> <p>I3 is a program for research cooperation involving 16 laboratories and institutions throughout Europe. This corresponds to the world largest network of synchrotron and FEL facilities.</p> <p><b>Web:</b> <a href="http://www.elettra.trieste.it/i3">http://www.elettra.trieste.it/i3</a></p>
	<p>European Microscopy Society (EMS)</p> <p><b>Web:</b> <a href="http://www.euremicsoc.org/index.html">http://www.euremicsoc.org/index.html</a></p>





## Major Sponsors

	<p><b>Elmitec Elektronenmikroskopie GmbH</b> Albrecht-von-Groddeck-Str. 3 38678 Clausthal-Zellerfeld Germany</p> <p><b>Phone:</b> +49 5323 1806 <b>Fax:</b> +49 5323 78932 <b>Email:</b> mail@elmitec.de <b>Web:</b> <a href="http://www.elmitec.de/">http://www.elmitec.de/</a></p>
	<p><b>SAES Getters S.p.A.</b> Viale Italia 77 20020 Lainate (Milan) - Italy</p> <p><b>Phone:</b> +39 02 93178 1 <b>Fax:</b> +39 02 93178 320 <b>Contact:</b> Mr. Paolo Manini Vacuum Systems Business Manager <b>Phone:</b> +39 02 93178284 <b>Email:</b> neg_technology@saes-group.com <b>Web:</b> <a href="http://www.saesgetters.com">www.saesgetters.com</a></p>
	<p><b>SPECS GmbH</b> Voltastrasse 5 D-13355 Berlin Germany</p> <p><b>Phone:</b> +49 30 46 78 24 0 <b>Fax:</b> +49 30 46 42 08 3 <b>Email:</b> support@specs.de, sales@specs.de <b>Web:</b> <a href="http://www.specs.de/">http://www.specs.de/</a></p>

## Sponsors

 <p><b>Gambetti</b> Vacuum Technology and Related Solutions</p>	<p><b>G. Gambetti Kenologia Srl</b> Via Volta 27 20082 Binasco (Milano), Italy</p> <p><b>Phone:</b> +39 02 90093082 <b>Fax:</b> +39 02 9052778 <b>Email:</b> sales@gambetti.it <b>Web:</b> <a href="http://www.gambetti.it/">http://www.gambetti.it/</a></p>
 <p><b>Omicron</b> NanoTechnology</p>	<p><b>Omicron NanoTechnology GmbH</b> Limburger Str. 75 65232 Taunusstein</p> <p><b>Phone:</b> +49 6128 987 230 <b>Fax:</b> +49 6128 987 33 230 <b>Email:</b> info@omicron.de <b>Web:</b> <a href="http://www.omicron-instruments.com/">http://www.omicron-instruments.com/</a></p>
 <p><b>PFEIFFER</b> VACUUM</p>	<p><b>Pfeiffer Vacuum Italia SpA</b> Via San Martino, 44 20017 Rho, Milan, Italy</p> <p><b>Phone:</b> +39 02 939905-23 <b>Fax:</b> +39 02 939905-33 <b>Email:</b> antonella.trentarossi@pfeiffer-vacuum.it <b>Web:</b> <a href="http://www.pfeiffer-vacuum.net/">http://www.pfeiffer-vacuum.net/</a></p>
 <p><b>Photek</b> <a href="http://www.photek.co.uk">www.photek.co.uk</a></p>	<p><b>Photek Ltd</b> 26 Castleham Road St Leonards on Sea East Sussex TN38 9NS United Kingdom</p> <p><b>Phone:</b> +44 (0)1424 850555 <b>Fax:</b> +44 (0)1424 850051 <b>Email:</b> sales@photek.co.uk <b>Web:</b> <a href="http://www.photek.co.uk/">http://www.photek.co.uk/</a></p>
 <p><b>STAIB INSTRUMENTS</b></p>	<p><b>Staub Instrumente GmbH</b> HagenauStrasse 22, D-85416 Lagenbach, Germany</p> <p><b>Phone:</b> +49 8761 76 240 <b>Fax:</b> +49 8761 76 24 60 <b>Email:</b> sales@staibinstruments.com <b>Web:</b> <a href="http://www.staibinstruments.com/">http://www.staibinstruments.com/</a></p>



 <p><b>Surface preparation</b> laboratory</p>	<p><b>Surface Preparation Laboratory</b>          Penningweg 69 F          1507 DE Zaandam          The Netherlands</p> <p><b>Phone:</b> +31-75-6120501  <b>Fax:</b> +31-75-6120491  <b>Email:</b> koper@surface-prep-lab.com  <b>Web:</b> <a href="http://www.surface-prep-lab.com/">http://www.surface-prep-lab.com/</a></p>
 <p><b>VACUUM SCIENCE</b></p> <p><small>exclusive Distributors of VG Scientia Ltd.          Thermo Fischer Scientific</small></p>	<p><b>Vacuum Science / VG Scientia</b>          Via G. Compagnoni, 37          20129 Milano</p> <p><b>Phone:</b> +39 0239664549  <b>Email:</b> luca.rimoldi@vacuumscience.it  <b>Web:</b> <a href="http://www.vgscienta.com/">http://www.vgscienta.com/</a></p>
 <p><b>vaqtec</b> vacuum technology &amp; components</p>	<p><b>Vaqtec S.r.l.</b>          Cso V. Emanuele II 25/B          12100 Cuneo - Italy</p> <p><b>Phone:</b> +39.0171.66507  <b>Fax:</b> +39.0171.64578  <b>Email:</b> info@vaqtec.com  <b>Web:</b> <a href="http://www.vaqtec.com/">http://www.vaqtec.com/</a></p>
 <p><b>5Pascal</b></p>	<p><b>Cinquepascal S.r.l.</b>          Via Carpaccio 35          20090 Trezzano sul Naviglio (Milano)          Italy</p> <p><b>Phone:</b> +39-02-4455-913          +39-02-4453-506  <b>Fax:</b> +39-02-4846-8659  <b>Email:</b> info@5pascal.it  <b>Web:</b> <a href="http://www.5pascal.it">www.5pascal.it</a></p>

## High-pressure Photoemission in Catalysis: Still new insights in well-studied systems?

Robert Schlögl

*Fritz Haber Institute of the Max Planck Society  
Faradayweg 4 – 6, D-14195 Berlin, Germany*

[www.fhi-berlin.mpg.de](http://www.fhi-berlin.mpg.de)

Surface analysis is conventionally confined to pressures at which emitted photoelectrons can travel over large distances. This limits the chemical extremely useful photoemission technique to low pressures at which only few catalytic reactions occur. Moreover, at these low pressures the catalyst operates in the limit of a surface-only mode in which only processes need to be considered occurring at the gas-solid interface.

At ambient or higher pressures multiple indications exist documenting the involvement of the sub-surface region of the catalytic material in the formation or deactivation of the surface-catalytic process. It is thus highly desirable to develop a method allowing the chemical analysis of the gas-solid interface at pressures under which the sub-surface chemistry is activated.

A synchrotron-based instrumentation has been developed in collaboration with the group of M Salmeron (Berkeley) for that purpose consisting of a very small sample chamber with an X-ray window and a small exit hole through which photoelectrons can enter a differentially pumped “electron microscope” operating for polychromatic electrons that images the hole into the inlet slit of a conventional hemispherical analyzer.

Examples of its operation will be discussed addressing simple catalytic reactions such as oxidation of CO and of methanol over coin metals and Ru. It will be shown that highly active states of these “simple” systems involve always sub-surface species. This observation is not confined to oxidation reactions and sub-surface oxygen but occurs also at hydrogenation reactions with sub-surface carbon moderating the chemical potential of surface hydrogen species.

### References

Teschner D, Borsodi J, Wootsch A, Revay Z, Hävecker M, Knop-Gericke A, et al. Science. 2008 Apr;320(5872):86-9.

## Transition metal oxidation – novel insights from in-situ low-energy electron microscopy

J. I. Flege<sup>1,4</sup>, F. Alamgir<sup>2</sup>, S. D. Senanayake<sup>3</sup>, P. Sutter<sup>4</sup>

<sup>1</sup>*Institute of Solid State Physics, University of Bremen, Bremen, Germany*

<sup>2</sup>*Georgia Institute of Technology, Atlanta, Georgia, United States*

<sup>3</sup>*Oak Ridge National Laboratory, Oak Ridge, Tennessee, United States*

<sup>4</sup>*Brookhaven National Laboratory, Upton, New York, United States*

Email: flege@ifp.uni-bremen.de

The oxides of late transition metals (TM), such as ruthenium, rhodium, and nickel, are a class of materials with desirable functional properties, e. g., for catalysis. However, the mechanism of initial oxidation of these materials and the nature of the structures produced by facile oxygen uptake into sub-surface layers have been notoriously difficult to investigate experimentally, primarily because of a lack of spatially resolving and structurally sensitive techniques adequate for identifying the initial nanometer-sized oxidation products under reaction conditions. Here we use spatially and temporally resolved structural fingerprinting in connection with multiple scattering calculations to characterize surface oxidation as well as the catalytic properties of the resulting oxygen-rich structures on Ru(0001) [1], Rh(111) [2], and Ni(111). We will show that for both Ru and Rh the initial oxidation proceeds by initial formation of a O-TM-O trilayer. While in the case of Rh [3] the thicker oxide structures emerge from the trilayer surface oxide, the bulk oxide RuO<sub>2</sub>(110) islands grow independently from the trilayer, competing for surface area (left figure). Depending on temperature, even a conversion from the ultra-thin RuO<sub>2</sub>(110) film to the trilayer-like surface oxide is observed. For Ni(111) oxidation, however, extended (1x1)-reconstructed trilayer formation is found for low temperatures, while for higher temperatures different reconstructions and oxygen-rich structures are identified [4].

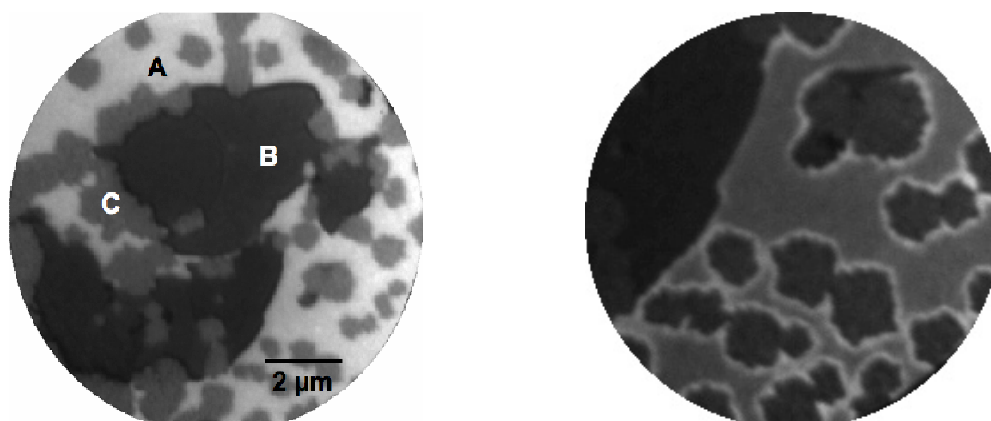


**Figure.** Left: LEEM image (field of view: 10  $\mu\text{m}$ ) of an oxidized Ru(0001) surface after exposure to NO<sub>2</sub>. The surface morphology consists of three distinct surface phases (A – (1x1)-O; B – RuO<sub>2</sub>(110); C – trilayer surface oxide). Right: Re-oxidation of the oxygen adlayer following CO exposure by spillover from trilayer domains (lower right corner from left image, field of view: 4.3  $\mu\text{m}$ ).

In the case of Ru, apart from the phase-specific chemical reactivities for CO oxidation, the presence of nanoscale heterogeneity also gives rise to *cooperative effects*, such as oxygen spillover, during the catalytic cycle, which can be followed under reaction conditions using LEEM (right figure).

### References

[1] J. I. Flege, J. Hrbek, and P. Sutter, *submitted*.

[2] J. I. Flege and P. Sutter, *submitted*.

[3] J. Gustafson et al., *Phys. Rev. Lett.* **92**, 126102 (2004).

[4] J. I. Flege, F. Alamgir, S. D. Senanayake, and P. Sutter, *in preparation*.

## Oxygen species on Ag(111) and the ethylene epoxidation reaction

Sebastian Günther<sup>1</sup>, Robert Reichelt<sup>1</sup>, Joost Winterlin<sup>1</sup>, Wolfgang Moritz<sup>2</sup>,  
Lucia Aballe<sup>3</sup>, Tevfik Mentès<sup>3</sup>, Alexej Barinov<sup>3</sup>, Miguel Nino<sup>3</sup>, Andrea Locatelli<sup>3</sup>

<sup>1</sup>LMU München, Department. Chemie, Butenandtstr.5-13 E, 81377 München, Germany

<sup>2</sup>LMU München, Institut für Kristallographie, München, Germany

<sup>3</sup>Sincrotrone Trieste S.C.p.A. SS 14 - km 163,5 in AREA Science Park 34012 Basovizza, Triest, Italy

Email: sebastian.guenther@cup.uni-muenchen.de

Due to their potential relevance in the ethylene epoxidation reaction we investigated oxygen species on Ag(111) under controlled conditions both at high pressure using O<sub>2</sub> and in UHV using NO<sub>2</sub> following a recipe described in [1]. After mounting a differentially pumped gas dosing system to the LEEM/XPEEM instrument at the nanospectroscopy beamline of ELETTRA we monitored the structure and morphology changes of the Ag(111) surface during the adsorption of NO<sub>2</sub>. Especially the formation of the (4x4)-O adsorption phase could be imaged in situ and it was found that surprisingly the nucleation and growth of this phase takes place on a mesoscopic length scale in the  $\mu\text{m}$  range. We used dark field imaging to identify the lateral distribution of the (4x4)-O phase and performed a full LEED I/V analysis of the adsorbate structure making use of the  $\mu$ -spot LEED acquisition mode of the LEEM instrument with an analysis area of  $\sim 2 \mu\text{m}$  diameter. In a separate experiment we repeated the measurements using a conventional LEED apparatus. The I/V analysis performed using the LEEM and the standard LEED were of similar quality as verified by comparing the I/V curves obtained from a clean Ag(111) surface. In the case of the (4x4)-O adsorbate phase the LEEM analysis provided significantly more spots for the I/V data set due to the accessibility of spots close to the (0,0) reflex. We were able to prove the structure model of the oxygen induced (4x4) surface reconstruction recently proposed in [2], while other models could be ruled out [3]. To our knowledge up to now a LEEM instrument has not been used for a successful structure analysis of a complex adsorbate structure. Meanwhile, we extended our investigations towards the preparation of further oxygen species on Ag(111). As can be seen in the figure below, at step bunches the amount of surface oxygen species may vary in a lateral inhomogeneous way. Using the imaging XPS mode of the XPEEM instrument at ELETTRA and performing  $\mu$ -spot XPS analysis we were able to characterize these further oxygen species.

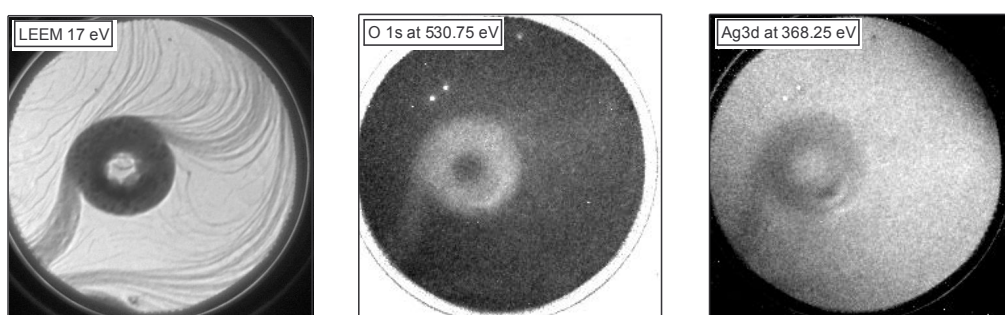


**Figure.** Lateral inhomogeneous oxygen accumulation at step bunches after adsorption of  $\alpha \times 210 \text{ L NO}_2$  at  $T=190^\circ\text{C}$ . (gas doser enhancement  $\alpha \sim 5\text{-}20$ ) Image size:  $(20 \mu\text{m})^2$

### References

- [1] S. R. Bare, K. Griffith, W. N. Lennard, H. T. Tang, Surf. Sci. 342, 185 (1995).
- [2] M. Schmidt et al., Phys. Rev. Lett. 96, 146102 (2006). and J. Schnadt et al., Phys. Rev. Lett. 96, 146101 (2006).
- [3] C. I. Carlisle, T. Fujimoto, W. S. Sim, D. A. King, Surf. Sci. 470, 15 (2000).

## Complex patterns in the NO + H<sub>2</sub> reaction on a K-promoted Rh(110) surface

S. Günther<sup>2</sup>, L. Hong<sup>1</sup>, A. Locatelli<sup>3</sup>, and R. Imbihl<sup>1</sup>

<sup>1</sup>*Institut für Physikalische Chemie und Elektrochemie, Leibniz-Universität Hannover, Callinstr. 3 – 3a, D-30167 Hannover, Germany*

<sup>2</sup>*LMU München Dept. Chemie, München, Germany*

<sup>3</sup>*Sincrotrone Trieste, Area Science Park-Basovizza, I-34012 Trieste, Italy*

Email: imbihl@pci.uni-hannover.de

The NO + H<sub>2</sub> reaction on a Rh(110) surface predosed with a submonolayer coverage of potassium exhibits a number of novel chemical wave phenomena: one observes pulses transporting potassium, a “spider web”-like wave patterns associated probably with a local modification of the surface, and one finds, in addition, stationary patterns and chemical turbulence. These wave patterns have been studied with LEEM/MEM,  $\mu$ -LEED, and SPELEEM (=spectroscopic LEEM)/ $\mu$ -XPS in the 10<sup>-7</sup> mbar range. The contribution of various ordered adlayers and of different chemical species to the wave patterns could be identified. Supported by realistic mathematical modeling a consistent mechanistic picture explaining the mass transport of K with the pulses was established. The mass transport is essentially due to strong energetic interactions of the alkali metal with the O,N-coadsorbates, i. e. the attraction of potassium to oxygen and an effective repulsion with the nitrogen adlayer [1].

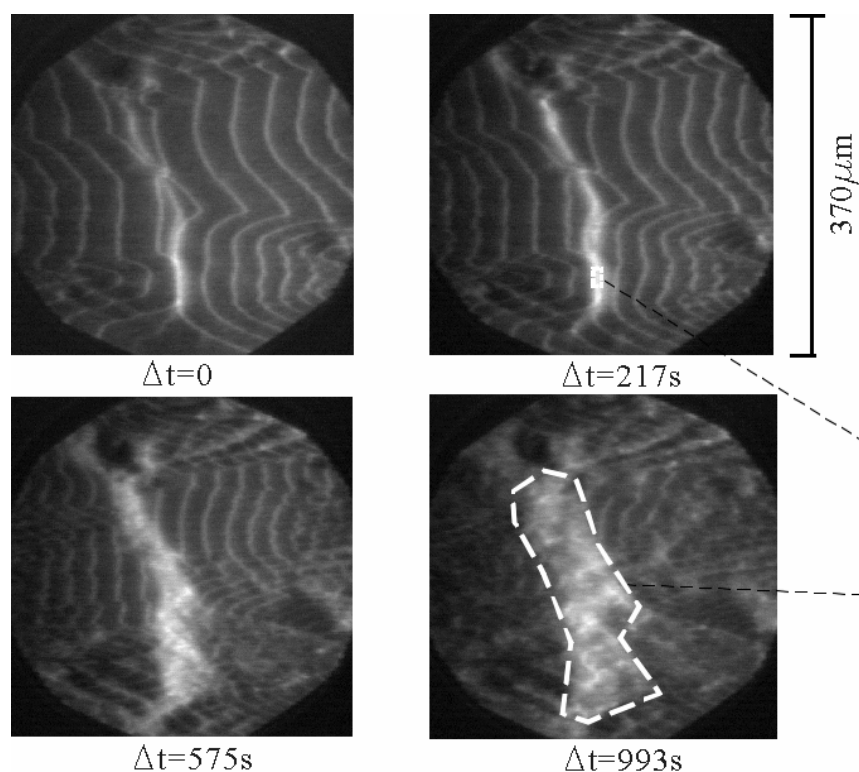


**Figure:** PEEM experiment demonstrating the enrichment of K in the collision area of two pulse trains.

### References

[1] Liu Hong, H. Uecker M. Hinz, Q. Liang, I.G. Kevrekidis, S. Günther, A. Locatelli, and R. Imbihl, submitted.



## ***In-situ* microscopic study of the interface-controlled growth of rubrene thin films**

Jerzy T. Sadowski<sup>1</sup>, Abdullah-Al-Mahboob<sup>2</sup>, Jun-Zhong Wang<sup>2</sup>, Yasunori Fujikawa<sup>2</sup>  
and Toshio Sakurai<sup>2</sup>

<sup>1</sup>*Center for Functional Nanomaterials, Brookhaven National Laboratory, Upton, NY 11973, USA*

<sup>2</sup>*Institute for Materials Research, Tohoku University, Sendai 980-8577, Japan*

Email: sadowski@bnl.gov

The pentacene (Pn: C<sub>22</sub>H<sub>14</sub>), has been studied extensively since it has a reasonable carrier mobility and has been successfully used in organic thin-film transistors (OTFT's). Now, the rubrene (5,6,11,12-tetraphenylanthracene: C<sub>42</sub>H<sub>28</sub>) is attracting a considerable attention since it has shown promise in OTFT's, with field-effect mobilities of the single-crystal FET devices surpassing that of amorphous silicon and even pentacene [1]. However, still little is known about the relation between the structural, chemical, and electrical properties of the substrate and the structure of the rubrene films.

We utilized *in-situ* low-energy electron microscopy (LEEM) and scanning tunneling microscopy (STM) to investigate the growth mode, crystallinity and morphology of the thin rubrene films deposited in ultra-high vacuum (UHV) conditions on clean, as well as modified Si substrates.

In case of rubrene deposition on a clean Si(111) surface at room temperature (RT), rubrene molecules react with the Si dangling bonds, partially dissociating and forming a wetting layer. On top of it, the crystalline islands nucleate, but a high nucleation density and rather poor surface diffusion, due to a rough and disordered interface result in a poor crystallinity of Rn film.

A completely different growth mechanism has been observed upon rubrene deposition on Bi(0001)

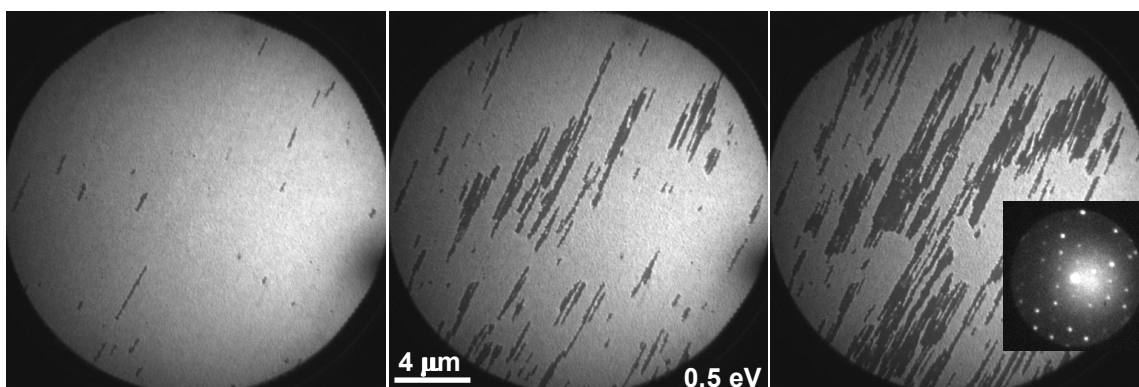


**Figure.** A series of the successive LEEM images (Field of view: 20μm) recorded during the deposition of rubrene (dark) on Bi(0001) surface (bright) at 400K; Rubrene islands are highly anisotropic and elongated along the substrate surface terraces; in the inset: μ-LEED pattern from a ML rubrene island on Bi(0001).

surface at RT. Rubrene islands nucleated on Bi(0001) surface immediately, without formation of a wetting layer. The morphology and crystallinity of the film was dramatically improved upon the rising the substrate temperature to 400K. In this case the nucleation of the large, single-crystalline rubrene grains, preferentially oriented along the surface terraces. Moreover, a LEED pattern indicated a formation of a new rubrene phase on Bi(0001) surface. In contrast to bulk phase (orthorhombic), the monolayer of rubrene on Bi(0001) had a hexagonal arrangements of the molecules. At coverages exceeding 5 ML, rubrene film has been observed to grow in 3D fashion, with nucleation of anisotropic, rectangular islands with shapes resembling those of rubrene single-crystal platelets.

### References

[1] V. C. Sundar et al., *Science* **303**, 1644 (2004).

## The growth mechanism of anisotropic pentacene heteroepitaxial films

A. Al-Mahboob<sup>1</sup>, J. T. Sadowski<sup>2,3</sup>, Y. Fujikawa<sup>2</sup>, R. M. Tromp<sup>1,4</sup> and T. Sakurai<sup>1</sup>

<sup>1</sup>WPI-Advanced Institute for Materials Research, Tohoku University

<sup>2</sup>Institute for Materials Research, Tohoku University

<sup>3</sup>Currently at CFN, Brookhaven National Lab, NY

<sup>4</sup>IBM TJ Watson Research Center, NY

The kinetically driven growth processes in pentacene (Pn) are found to be modified essentially by the anisotropy in the molecular and crystal structures [1,2] but it cannot be predicted directly from the competitive equilibrium processes. We observed a (001) oriented Pn film growth even after stopping deposition on semiconducting or semi-metallic surfaces indicating long diffusion time in contrast to the growth of Pn on SAM, oxide or wetting layer on clean silicon surfaces. The long diffusion time could be due to large barrier for orienting standing up from lying Pn molecules during diffusion on surfaces caused by stronger interaction while the diffusion time is smaller on more inert surfaces. If the barrier is higher further, the growth becomes more complicated as we observed in the growth of Pn on fullerene (C<sub>60</sub>). Here we will discuss mainly the growth mechanism of Pn-C<sub>60</sub> heteroepitaxial films studied by real time low-energy electron microscopy.

Pn and C<sub>60</sub> are of great interest among organic semiconductors as they show highest field-effect hole and electron mobilities respectively and thus a Pn-C<sub>60</sub> heterostructure can be a promising candidate for donor-accepter based organic devices. We observed a competitive growth between a thin-film phase of Pn having tilted standing-up orientation and a new phase with laying-down orientation. The growth of laying-down phase at room temperature is suppressed gradually with increasing film thickness. The nucleation of this phase is also suppressed with increasing temperature indicating that the thermal activation against barrier of diffusing molecule helps Pn molecules to be standing up in film growth. At the intermediate temperature we observed two distinct types of nucleation – an earlier nucleation of lying down phase and a delayed nucleation of standing-up phase. The standing up phase without co-presence of laying down phase could be achieved at ~70°C.

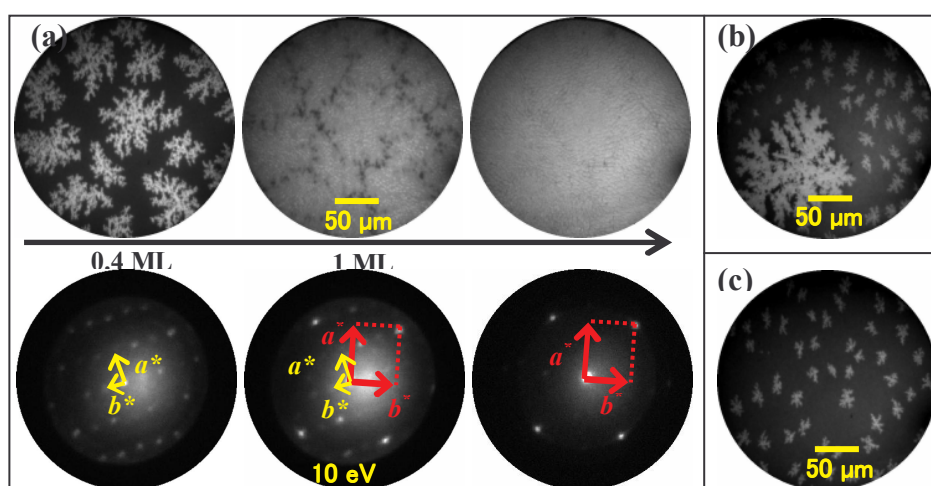


**Fig. 1.** LEEM images showing growth of Pn on C<sub>60</sub> at various temperatures: (a) Time series LEEM images during growth at RT and the corresponding LEED patterns recorded from a Pn island, unit cell vectors of lying down and standing-up Pn phases are outlined by yellow and red arrows respectively; (b) Growth at ~65 °C, nucleation of lying down phase (large island) and a delayed distinct nucleation of standing-up phase (smaller islands) have been observed; (c) Growth of standing-up Pn phase at ~75 °C without co-presence of lying down phase.

### References

- [1] J. T. Sadowski et al 2007, *Phys. Rev. Lett.* 98, 046104  
 [2] A. Al-Mahboob et al 2008, *Phys. Rev.* B77, 035426

## Band structure theory of very low energy electron diffraction and final states effects in photoemission

Eugene Krasovskii

<sup>1</sup>Institute of Metal Physics, National Academy of Sciences of Ukraine, 03142 Kiev, Ukraine

<sup>2</sup>Institut für Theoretische Physik und Astrophysik, Universität Kiel, D-24098 Kiel, Germany

Email: krasovsk@theo-physik.uni-kiel.de

Very low energy electron diffraction (VLEED) and angle-resolved photoemission (ARPES) are complementary methods to study electronic structure of solids. However, even for periodic solids, to extract the information from the experiment is not straightforward because of the complex relation between the measured spectra and the underlying band structure. In this talk an *ab initio* theory of VLEED and ARPES is presented within the Bloch waves approach to electron scattering. It is based on an embedding technique formulated in the augmented plane waves formalism [1]. In this method the substrate is represented by its *complex band structure* (CBS) and the scattering region by a basis set expansion.

Experimental VLEED spectra of layered chalcogenides NbSe<sub>2</sub> and TiTe<sub>2</sub> and graphite will be analysed. Special attention will be payed to the phenomenological description of inelastic effects.

In the one-step theory of photoemission [2] the outgoing electron is described by a time-reversed LEED state. This establishes theoretical grounds for *band mapping*: deriving the quasi-particle band structure from a surface sensitive ARPES experiment, see Figure. Interference between Bloch constituents of the photoelectron initial and final states in the presence of inelastic scattering is discussed. Its implications for band mapping and for determining the lifetimes of initial and final states are demonstrated on surface states photoemission from Al, Cu, and Be, as well as valence band photoemission from Al [3] and TiTe<sub>2</sub> [4]. Band mapping by a two-photon photoemission will be discussed; an example for Si(100) surface will be presented.

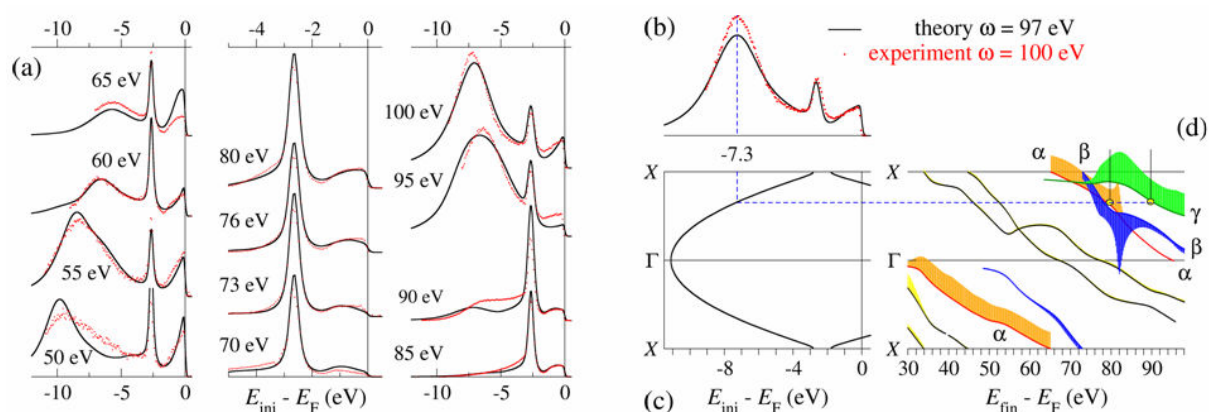


**Figure.** Band structure analysis of normal emission photoelectron energy distribution curves (EDC) for Al(100). (a) Theoretical (lines) and measured (dots) EDCs [3] for photon energies 50-100 eV. (b) Calculated EDC for  $\omega=97$  eV compared to the measured spectrum (dots) for  $\omega=100$  eV. (c) Band structure along the  $X\Gamma X$  line; direct transitions from  $E_{ini}=-7.3$  eV to the CBS branches  $\alpha$  and  $\gamma$ . (d) The Bloch wave decomposition of the LEED states: current carried by individual waves is shown by the vertical extent of the shaded area.

### References

- [1] Krasovskii E E 2004 *Phys. Rev. B* 70, 245322
- [2] Feibelman P J, Eastman D E 1974 *Phys. Rev. B* 10, 4932
- [3] Krasovskii E E, Schattke W, Jiřiček P, et al to be published
- [4] Krasovskii E E, Rossnagel K, Fedorov A, Schattke W, Kipp L, 2007 *Phys. Rev. Lett.* 98, 217604



## Correlation of the electronic structure and surface oxidation of ultrathin Al films

L. Aballe<sup>1</sup>, A. Barinov<sup>2</sup>, N. Binggeli<sup>3,4</sup>, N. Stojic<sup>4,5</sup>, T.O. Mentès<sup>2</sup>, A. Locatelli<sup>2</sup>, M. Kiskinova<sup>2</sup>

<sup>1</sup> CELLS- ALBA Synchrotron Light Facility, C3 Campus UAB, 08193 Bellaterra, Barcelona, Spain

<sup>2</sup> Sincrotrone Trieste S.C.p.A., Basovizza-Trieste 34012, Italy

<sup>3</sup> Abdus Salam International Centre for Theoretical Physics, Strada Costiera 11, Trieste 34014, Italy

<sup>4</sup> Theory @ Elettra Group, INFN-CNR Democritos, Trieste I-34014, Italy

<sup>5</sup> Scuola Internazionale Superiore di Studi Avanzati (SISSA), Via Beirut 2-4, Trieste I-34014, Italy

Email: lucia.aballe@cells.es

The effect of electron quantum confinement on the surface reactivity of ultrathin metal films is explored by comparing the initial oxidation rate of atomically flat Aluminum films of different thickness, using complementary microscopy techniques. The growth morphology of Al films on W(110) is characterized by LEEM and micro-spot LEED, in order to optimize the growth conditions and to select appropriate surface areas for spectroscopy. The electronic structure and surface oxidation of well known atomic thickness are measured by synchrotron XPEEM and micro-spot photoelectron spectroscopy, on the valence band and Al2p core level.

As in the case of Mg films [1], layer dependent oscillations of the surface reactivity are found, in correlation with the electronic quantum well states resulting from the confinement of quasi-free valence electrons in the metal film. Roughly, there is a maximum in reactivity each time a quantum-well state crosses the Fermi level, increasing the local density of electronic states. A closer look and comparison with first principle calculations point however to a dominating role of the electron density decay length in vacuum, as previously suggested by theory [2,3]. The effect of the substrate is found to be of uttermost importance for the subtleties of the surface electronic structure, stressing the need of understanding the electronic coupling at the interface.

### References

- [1] L. Aballe, A. Barinov, A. Locatelli, S. Heun, and M. Kiskinova, Phys. Rev. Lett. 93, 196103 (2004)
- [2] A. Hellman, Phys. Rev. B 72, 201403 (2005)
- [3] N. Binggeli and M. Altarelli, Phys. Rev. Lett. 96, 036805 (2006)

## Molecular and electronic structure of hydrogen-bond stabilized organic domains

Fawad S. Khokhar, Raoul van Gastel and Bene Poelsema

*MESA<sup>+</sup> Institute for Nanotechnology, Solid State Physics,  
University of Twente, P.O. Box 217, 7500 AE, Enschede, The Netherlands*

Email: [f.s.khokhar@tnw.utwente.nl](mailto:f.s.khokhar@tnw.utwente.nl)

Organic two-dimensional nanostructures can be used for nanopatterning of substrates, heterogeneous catalysis, sensing and molecular recognition, etc. [1]. We have used Low Energy Electron Microscopy (LEEM) to study the growth of hydrogen-bond stabilized organic domains. The ability of LEEM to perform real-time, in-situ imaging at high resolution and low electron energies makes it a unique tool to study growth processes of these structures [2]. We have grown 4,4'-biphenyldicarboxylic acid (BDA) domains on a Cu(001) surface. The phenyl rings in this organic molecule lead to a flat adsorption geometry of the molecule on the surface. The carboxylic acid end groups form intermolecular hydrogen bonds [3] that are responsible for the in-plane structure of the domains.

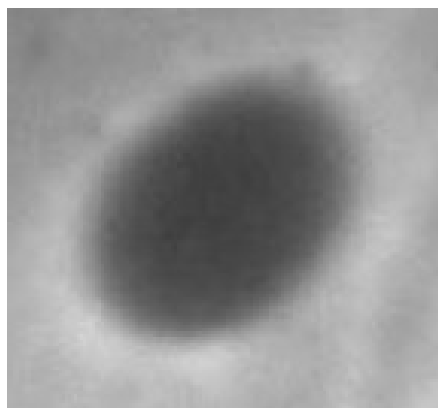


**Figure 1:** LEEM image of a BDA domain showing a halo at an electron energy of 2.5 eV. Field of view is 1.4 microns.

We have observed the initial nucleation and growth of BDA domains as well as the temporal evolution of the domains at several temperatures. Our LEEM data (figure 1) shows rings of bright intensity (a.k.a. halos) surrounding the domains at low electron energies. A simple analysis of the intensity profile in the vicinity of the BDA domains from LEEM I-V curves shows that a significant work function difference exists between solid domains and the 2D gas phase of BDA molecules on the adjacent terraces. The interpretation of the intensity profiles is not straightforward. The domains exhibit variations in molecular and electronic structure in the interior of the domain, which leads to intensity variations inside as well as outside the domains. We use both LEEM I-V curves and coverage dependent variations in scattering cross-section to interpret our observations. The latter recipe is taken from He atom scattering and indicates that the distribution of BDA

molecules in the domains is rather non-uniform. Preliminary results lead us to propose that the BDA domains are not compact, but dendritic in nature.

### References

- [1] S. Stepanow, N. Lin, F. Vidal, A. Landa, M. Ruben, J.V. Barth, and K. Kern, *NanoLett.* 5, 901(2005).
- [2] R. J. Phaneuf and A. K. Schmid, *Phys.Today* 56, 50 (2003).
- [3] J.V. Barth, J. Weckesser, N. Lin, A. Dmitriev and K. Kern, *Appl. Phys. A* 76, 645 (2003).

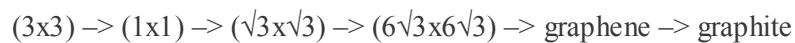
## Morphology and Electronic Structure of Thin Graphene Films on SiC

R.M. Tromp, J.B. Hannon

*IBM T.J. Watson Research Center, 1101 Kitchawan Road,  
P.O. Box 218, Yorktown Heights, NY 10598, USA*

Email: [rtromp@us.ibm.com](mailto:rtromp@us.ibm.com)

It is well known that thin epitaxial graphene films form on 6H and 4H SiC(0001) surfaces upon high temperature annealing, following an elaborate sequence of phase transformations from low to high temperature:



In our experiments, we prepare clean, ordered SiC surfaces with highly regular atomic step arrays. The initial surface morphology, with atomic steps corresponding to a single SiC double layer, transforms to a triple-layer morphology (on 6H-SiC(0001)) upon annealing. Through the  $(\sqrt{3} \times \sqrt{3})$  phase this highly ordered surface morphology is maintained, but formation of the  $(6\sqrt{3} \times 6\sqrt{3})$  phase is kinetically hindered, and pits are seen to form on the surface, with depths often exceeding 10 nm. Upon subsequent growth of graphene these pits persist.

The electronic structure of the surface is studied by in-situ Angle-Resolved Ultraviolet Photoelectron Spectroscopy (ARUPS), using the energy-filtered PEEM real space and reciprocal space imaging capability of the IBM LEEM instrument. On a single monolayer of graphene, we observe the  $\sigma$  and  $\pi$  bands as expected, with well defined Dirac points at or near the Fermi level (see figure). On the  $(6\sqrt{3} \times 6\sqrt{3})$  surface however, the  $\sigma$  bands are still observed, but the  $\pi$  bands are much less clearly defined, and the Dirac points virtually absent. At the same time, the  $(6\sqrt{3} \times 6\sqrt{3})$  LEED pattern is indicative of a graphene monolayer adsorbed onto SiC(0001). We conclude that the atomic structure is indeed that of a graphene-like layer on SiC(0001), with strong  $\sigma$  bonds in the plane, but with the  $\pi$  band disturbed by covalent bonding of atoms in the graphene-like sheet with the underlying substrate.

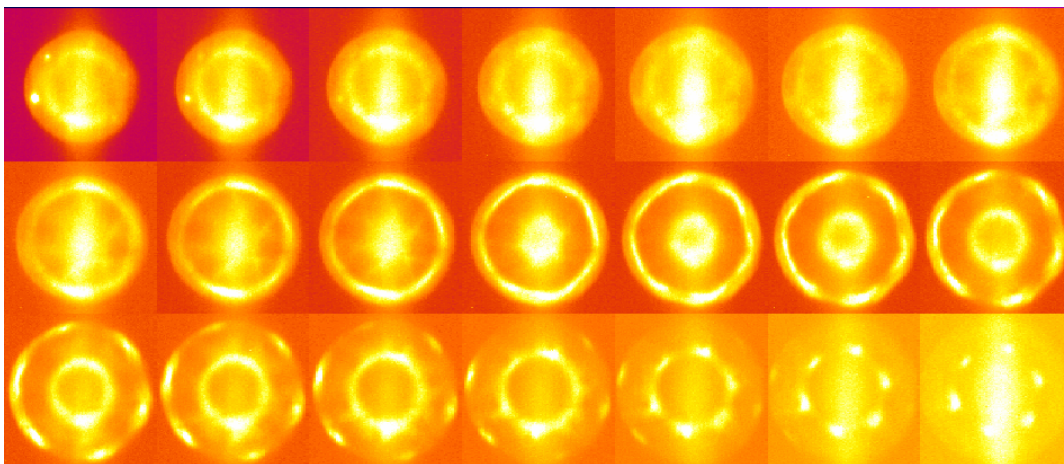


**Figure .** HeII photoelectron angular distributions for 1 ml graphene on SiC(0001). In the last few frames the Dirac points are easily discerned.

## Spectro-microscopy of single and multi-layer graphene supported by a weakly interacting substrate

Kevin R. Knox<sup>1,2</sup>, Shancai Wang<sup>2</sup>, Alberto Morgante<sup>3,4</sup>, Dean Cvetko<sup>3,5</sup>, Andrea Locatelli<sup>6</sup>,  
Tevfik Onur Mentesh<sup>6</sup>, Miguel Angel Niño<sup>6</sup>, Philip Kim<sup>1</sup>, R. M. Osgood Jr.<sup>2</sup>

<sup>1</sup> Department of Physics, Columbia University, New York, New York 10027, USA

<sup>2</sup> Department of Applied Physics, Columbia University, New York, New York 10027, USA

<sup>3</sup> Laboratorio TASC-INFM 34012, Basovizza, Trieste, Italy

<sup>4</sup> Department of Physics, Trieste University, Trieste, Italy

<sup>5</sup> Faculty for Mathematics and Physics, University of Ljubljana, Ljubljana, Slovenia.

<sup>6</sup> Elettra - Sincrotrone Trieste S.C.p.A., 34012 Basovizza, Trieste, Italy

Email: osgood@columbia.edu

While graphene's distinctive Dirac-cone electronic structure and simple 2D atomic structure have attracted major interest in the physics community, inherent limitations in the size of available exfoliated graphene samples have made it difficult to study such systems with typical UHV probes such as photoemission and low energy electron diffraction (LEED). Exfoliated graphene on SiO<sub>2</sub> is the system of choice for the majority of transport experiments[1,2]; however, all photoemission and LEED/LEEM studies of graphene performed thus far have probed films grown on SiC [3,4,5]. Using the high spatial resolution of the Nanospectroscopy beamline at the ELETTRA synchrotron light source, we have overcome such size limitations to study exfoliated graphene with micro-spot low energy electron diffraction ( $\mu$ LEED) and micro-spot angle resolved photoemission ( $\mu$ ARPES).

In this talk, we will discuss our measurements of the electronic structure and surface morphology of exfoliated graphene using  $\mu$ ARPES and  $\mu$ LEED/LEEM. Changes in LEEM contrast with layer thickness can be used to unambiguously determine film thickness, while LEED measurements provide information about the surface morphology of the graphene sheets, which is observed to change with layer thickness. Our photoemission measurements probe the unique massless fermionic dispersion of monolayer graphene.

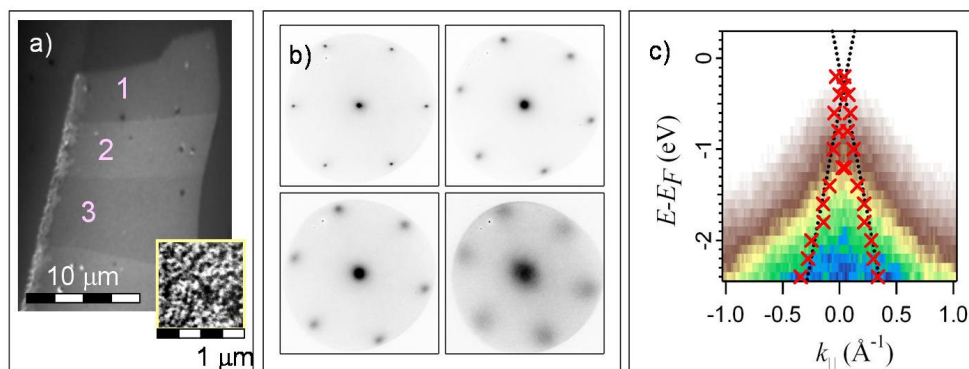


**Figure.** a) LEEM image of multilayer graphene sample (numbers indicate thickness in ML). Inset: high resolution LEEM image reveals microscopic corrugations in graphene. b) LEED images of graphite, trilayer, bilayer and monolayer graphene, respectively. c) Angle resolved photoemission intensity on monolayer graphene through K point in  $\Gamma M$  direction.

### References

- [1] K.S. Novoselov *et al.*, Science **306**, 666 (2004).
- [2] Y.B. Zhang *et al.*, Nature **438**, 201 (2005).
- [3] T. Ohta *et al.*, Science **313**, 951 (2006).
- [4] A. Bostwick *et al.*, Nature Physics **3**, 36 (2007).
- [5] S.Y. Zhou *et al.*, Nature Physics **2**, 595 (2006).

## Characterization of Ag microstructure using LEEM/PEEM spectromicroscopy

Y. Fujikawa<sup>1</sup>, T. Sakurai<sup>1</sup>, R. M. Tromp<sup>2</sup>

<sup>1</sup> Institute for Materials Research, Tohoku University, 2-1-1 Katahira, Aoba-ku, Sendai 980-8577, Japan

<sup>2</sup> IBM Research Division, T. J. Watson Research Center, 1101 Kitchawan Road, P.O. Box 218, Yorktown Heights, NY 10598

Email: fujika-0@imr.tohoku.ac.jp

Low energy electrons have been applied successfully for both structural and spectroscopic studies since the early days of modern surface science. While reciprocal space analysis has been combined with both microscopic and spectroscopic studies, there is still very limited availability of spectromicroscopic analysis because it is not easy to achieve both high spatial and spectroscopic resolution at low energies.

We present spectromicroscopic characterization of Ag islands on Si substrates using a newly developed energy-filtered Low Energy / Photoelectron Emission Microscope capable of 5D (2D spatial + 2D reciprocal + energy) surface analysis. The electron energy loss signal from Ag surface plasmons (SP) was imaged in real space with a resolution of 35 nm or less, while the SP energy dispersion spectra were obtained from a 6  $\mu\text{m}$  diameter area on Ag(111) within  $\sim 1$  second. [1] HeI (21.2 eV) photoemission spectra were obtained from a complex Ag island, selecting Ag(111) and Ag(100) areas with a  $\phi 4$   $\mu\text{m}$  aperture during PEEM observation. Full dispersion data covering the full reciprocal-energy space were obtained from both surfaces, reflecting their respective symmetries. The photoelectron distributions in the reciprocal space sliced at the strongest resonance peak at the d-band (Figure) indicate that the resonance takes place at the projections of bulk L points. The lack of 6-fold component at the edge of surface Brillouin zone in the Ag(111) spectra implies the missing of surface scattering/diffraction processes when photoelectrons pass through the surface potential. Detailed analysis of the Ag(111) spectra reveals that the surface scattering channel is activated for the photoelectrons with total reflection condition at the surface potential.

The ability to perform detailed spectromicroscopic experiments in a standard lab environment presented in this work is of key importance for nanoscale analysis of novel structures and materials.

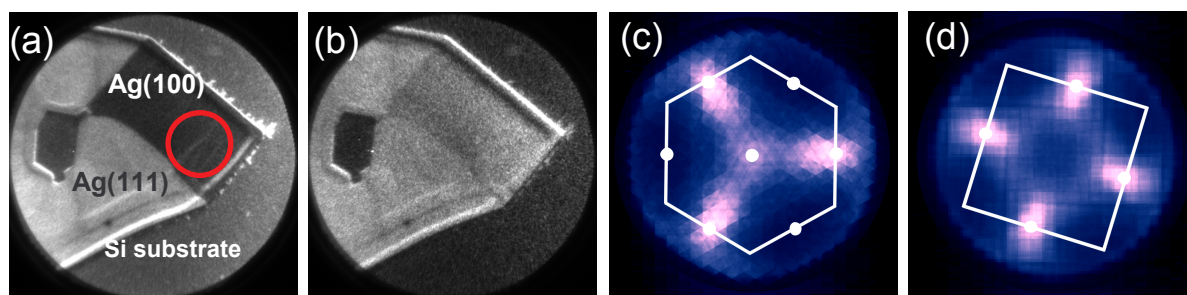


**Figure.** Energy-filtered PEEM images of a Ag island on Si(111) obtained from (a) secondary electrons and (b) d-band electrons (16  $\mu\text{m}$  field of view). The secondary electron image gives distinctive contrast due to final state effect. The aperture size of area-selection for spectroscopy mode is superimposed on the Ag(100) area (red circle). Energy slice images of photoelectrons at the L resonance distributed in the projection of Ewald sphere on the 2D reciprocal space are reconstructed from 22 E-k spectroscopic images, selecting (c) Ag(111) and (d) Ag(100) areas. The images are symmetrised following the observed symmetries by overlapping the rotated images. White lines and dots represent the surface Brillouin zone edges and projection of bulk L points, respectively.

### References

[1] Fujikawa Y, Sakurai T, and Tromp RM, 2008 *Phys. Rev. Lett.* 100, 126803



## Coordination effects in magnetic nanostructures

Carlo Carbone

*Istituto di Struttura della Materia.- Consiglio  
Nazionale delle Ricerche*

Email: [carlo.carbone@trieste.ism.cnr.it](mailto:carlo.carbone@trieste.ism.cnr.it)

Advanced synchrotron radiation techniques are able to provide high sensitivity to the study of very diluted magnetic systems, unveiling thus novel properties hardly accessible by other experimental techniques. X-ray circular dichroism, in particular, has been successfully used to track the evolution of the magnetic properties in nanostructures constructed at surfaces, from finite-sized particles to isolated adatoms. This presentation will illustrate how x-ray circular magnetic dichroism carried out in high magnetic fields and cryogenic conditions can be employed to simultaneously measure the valence state and magnetic moment of individual atoms and small clusters on surfaces. The results show how Hund's rule magnetic moments of a free atom change upon adsorption on a surface, the appearance of magnetic anisotropy, the dependence of the magnetic and electronic configuration on the substrate interaction and the atomic coordination.

## Spin reorientation transition in ultrathin Fe films on W(110)

Ryszard Zdyb<sup>1,2</sup>, Ernst Bauer<sup>1</sup>

<sup>1</sup>Department of Physics, Arizona State University, Tempe, Arizona, 85287-1504, USA

<sup>2</sup>Institute of Physics, Maria Curie-Skłodowska University, Pl. M. Curie-Skłodowskiej 1, 20-031 Lublin, Poland

Email: zdybr@hektor.umcs.lublin.pl

The structure and magnetism of ultrathin Fe films grown on 2 monolayers (ML) Au on a W(110) substrate are investigated with spin polarized low energy electron microscopy (SPLEEM). Depending upon deposition temperature  $T_d$  the Fe layer becomes magnetic at room temperature either at submonolayer coverages ( $T_d=700$  K) or at 1.55 ML ( $T_d=300$  K). The high temperature deposition results in an appearance of huge magnetic domains with the in-plane easy axis pointing in the  $[1\bar{1}0]$  direction [1]. Subsequent room temperature deposition on the top of 1 ML does not change the magnetic structure of the layer up to at least 10 ML. When Fe is deposited from the very beginning at room temperature also huge magnetic domains appear at 1.55 ML with the easy axis in the  $[1\bar{1}0]$  direction but right after the onset of magnetic order, at about 1.67 ML, new, small domains appear with the easy axis parallel to the  $[001]$  direction. Detailed analysis of the magnetization direction indicates that the easy axis rotates from the  $[1\bar{1}0]$  direction at the very beginning towards  $[001]$ , being most close to it (about  $10^\circ$  off  $[001]$ ) between 2 and 4 ML. Thereafter it rotates back towards the  $[1\bar{1}0]$  direction, deviating by about  $25^\circ$  from the  $[001]$  direction at about 7 ML. Finally it rotates again towards the  $[001]$  direction in which it remains for larger thicknesses.

The observed changes of the direction of the easy axis have been associated with changes in the crystallographic structure and morphology of the Fe layer. In the initial growth stage the Fe layer has *fcc* structure with the lattice constant of the 2 ML Au substrate. With increasing thickness Fe undergoes a structural transition to a *bcc* phase resulting in a decrease of the lattice constant. In addition, the *bcc* Fe layer develops a two-dimensional lattice of misfit dislocation which apparently influences the magnetic properties of the film.

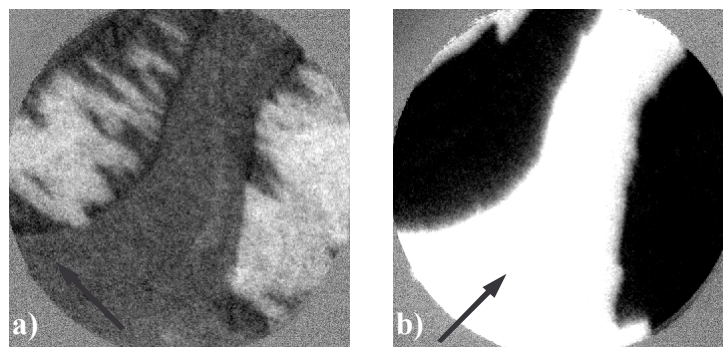


**Figure.** SPLEEM images of a Fe layer grown on 2 ML Au/W(110) at a thickness of 6 ML. The polarization vector of the electron beam is indicated by the arrows parallel to the  $[1\bar{1}0]$  a) and  $[001]$  b) directions. Field of view 14 microns. Electron energy 3.5 eV.

### References

[1] Zdyb R, Bauer E, 2008, *Phys. Rev. Lett.* 100, 155704.

## Surface Electron Microscopy studies of perfectly flat films: coinage metals and Co on Ru(0001)

Farid El Gabaly<sup>1</sup>, Arantzazu Mascaraque<sup>2</sup>, T. Onur Mentès<sup>3</sup>, Kevin F. McCarty<sup>4</sup>,  
Andrea Locatelli<sup>3</sup>, Andreas K. Schmid<sup>1</sup>, Juan de la Figuera<sup>5,6</sup>

<sup>1</sup>Lawrence Berkeley National Laboratory, Berkeley CA 94720, USA

<sup>2</sup>Universidad Complutense de Madrid, Madrid 28040, Spain

<sup>3</sup>Elettra Sincrotrone Trieste S.C.p.A., Trieste, Italy

<sup>4</sup>Sandia National Laboratories, Livermore CA 95440, USA

<sup>5</sup>Instituto de Química-Física Rocasolano, CSIC, Madrid 28006, Spain

<sup>6</sup>Universidad Autónoma de Madrid, Madrid 28049, Spain

Email: [juan.delafiguera@iqfr.csic.es](mailto:juan.delafiguera@iqfr.csic.es)

The magnetic properties of thin films result from a delicate balance of many contributions. Because of this, the magnetization can be very sensitive to small changes in properties such as film roughness and thickness. For example, the magnetization can change dramatically with the addition or removal of a single layer of film atoms. Given this strong dependence, methods that can simultaneously determine the local atomic thickness and the local magnetization are desirable. Surface electron microscopies allow this level of detail. In particular, both spin-polarized low energy electron microscopy (SPLEEM) and X-ray magnetic dichroism with photoexcited electron microscopy (XMCD-PEEM) are available for magnetic studies.

The current lateral resolution of most surface electron microscopes is about 10nm. For ready characterization, having films that are uniformly thick over substantially longer length scales are required. But in strained systems, layer-by-layer thin film growth is unstable towards the formation of 3-dimensional islands, which form to relieve the lattice mismatch with the substrate. We have developed an approach that avoids 3D island formation and yields uniformly thick films -- by depositing the film material on very large, atomically flat substrate terraces, layer-by-layer growth can proceed to relatively thick films (tens of layers), even when the lattice mismatch is in the range of 5-7% [1].

We report on SPLEEM and XMCD-PEEM observations of extremely flat Co thin films on Ru(0001). In addition to the bare films [1,2], we also focus on the growth of capping overlayers of non-magnetic coinage metals (Cu, Ag, Au). The different coinage metals present extremes in terms of lattice mismatch with the Co film, from a nearly lattice match for Cu/Co to a large mismatch that is accommodated by dislocations in Ag and Au on Co.

For selected combinations of overlayer and magnetic film thickness, we find that changing thickness of the non-magnetic capping metal even by a single atomic layer changes the easy-axis of the magnetization of the Co film. We will discuss the physical origins of the role of the capping layer in the magnetization.

This research was supported by the Office of Basic Energy Sciences, Division of Materials Sciences, U.S. Department of Energy under Contract No. DE-AC04-94AL85000, by the Spanish Ministry of Science and Technology through Project No. MAT2006-13149-C02-02.

### References

- [1] Farid El Gabaly et al. 2007 *New J. of Phys.* 9 80 (2007).
- [2] Farid El Gabaly et al. 2006 *Phys. Rev. Lett.* 96 147202 (2006).
- [3] Farid El Gabaly et al. 2008, arxiv 0804.4777.



## Application of x-ray spectromicroscopy to the study of magnetic properties of single nanoparticles

A. Fraile Rodríguez<sup>1</sup>, F. Nolting<sup>1</sup>, A. Kleibert<sup>2</sup>, and J. Bansmann<sup>3</sup>

<sup>1</sup>Swiss Light Source, Paul Scherrer Institut, CH 5232 Villigen, Switzerland

<sup>2</sup>Institute of Physics, Universität Rostock, D 18051 Rostock, Germany

<sup>3</sup>Department of Surface Chemistry and Catalysis, Universität Ulm, D 89069 Ulm, Germany

Email: arantxa.fraile-rodriguez@psi.ch

Magnetic nanoparticles show a variety of unusual magnetic phenomena when compared to the bulk materials, mostly due to the effect of the surface and interface on the magnetic interactions and to critical magnetic length scales such as domain wall width and exchange length. In most experiments, magnetic investigations are performed on assemblies of particles on mm<sup>2</sup>-areas. Since in these arrays the particles are often randomly distributed with regard to their crystallographic orientation and (or) magnetic easy axes, many complications arise when trying to deduce the magnetic properties of the individual particles from measurements of their collective behavior. Therefore, single-particle experiments are crucial in order to give a deeper and consistent insight into the scaling laws at the nanoscale. At the Swiss Light Source we have demonstrated the feasibility of PEEM for x-ray imaging and absorption spectroscopy of individual Co particles in the size range of 8 to 12 nm. For ex-situ (uncapped) samples, significant variations in the x-ray absorption spectra among different single cobalt particles were found [1]. Furthermore, distinctive spectral information of the single particles cancels out and cannot be detected in the measurement of an ensemble [1]. The x-ray PEEM data are correlated with scanning electron microscopy observations of the same particles in order to determine the size and aspect ratio of each particle in the ensemble. Currently we explore the capabilities of PEEM to assess particle-to-particle variations of key intrinsic properties such as the saturation magnetization and the magnetic anisotropy energy employing x-ray magnetic circular dichroism (XMCD). Recently, we obtained the first unambiguous observation of XMCD contrast from individual Fe particles in a size range of 5 to 25 nm deposited on ferromagnetic surfaces. Our initial results indicate a spatial distribution of the easy anisotropy axes of the individual particles in the ensemble.

### References

[1] A. Fraile Rodríguez, F. Nolting, J. Bansmann, A. Kleibert, L. J. Heyderman, J. Magn. Mag. Mat. (2007) **316**, 426.

## Imaging of exchange bias in Co/FeMn bilayers on the nm length scale

Florian Kronast<sup>1</sup>, Joachim Schlichting<sup>1</sup>, Alexey Rzhevskiy<sup>2</sup>, Florin Radu<sup>1</sup>, Mishra Shrawan<sup>1</sup>,  
Hermann A. Dürr<sup>1</sup> and Wolfgang Eberhardt<sup>1</sup>

<sup>1</sup>*BESSY GmbH, Berlin, Germany*

<sup>2</sup>*Freie Universität Berlin, Germany*

Email: kronast@bessy.de

Here we report on the first attempt to investigate the magnetic interface coupling in Co/FeMn bilayers by photoemission electron microscopy (PEEM) using applied magnetic fields during imaging. Recent PEEM studies of Co/FeMn bilayers could provide deeper insight into the arrangement of magnetic moments near the interface by element specific magnetic imaging [1]. They exhibit the presence of uncompensated Fe and Mn spins at the interface of the antiferromagnet [1]. So far PEEM studies could only be done at remanence. However, experiments in an applied saturating magnetic field on similar systems indicate that the exchange bias is most likely caused by a small fraction of uncompensated spins pinned to the antiferromagnet while the majority of spins follow the ferromagnetic layer [2], i.e. the external field. Due to the lack of spatial resolution in these experiments [2] the origin of the pinning could not be revealed so far.

In this PEEM study we investigated the domain structure in the ferromagnetic Co layer and the arrangement of magnetic moments at the interface of the antiferromagnet as a function of applied magnetic field. At the SPEEM endstation at BESSY a special sample holder with integrated magnetization yoke allowed us to apply magnetic fields up to 25mT without significant reduction of the spatial resolution. Analyzing the hysteresis loop of each pixel in the recorded images we could obtain a map of the local exchange bias displaying the shift of the hysteresis loop in the ferromagnetic Co layer. Our main objective is to correlate the observed variations in the local exchange bias with the magnetic arrangement of spins at the interface of the antiferromagnet. Saturating the ferromagnetic layer by the applied magnetic field we can probe the existence of uncompensated pinned spins at the interface of the antiferromagnet which are expected to be essential for the exchange bias.

### References

- [1] W. Kuch et al., PRB 75, 224406 (2007)
- [2] H. Ohldag et al., PRL 91, 017203 (2003)

## Antiferromagnetism vs. Paramagnetism: Revisiting the magnetostructure of MnAs on GaAs

Souliman El Moussaoui<sup>1,2</sup>, Rachid Belkhou<sup>1,2</sup>, Francesco Maccherozzi<sup>1,2</sup>, Ernst Bauer<sup>3</sup>,  
Nicolas Rougemaille<sup>4</sup>, Antoine Barbier<sup>5</sup>, Stefan Stanescu<sup>1</sup>,  
Fumiyoshi Takano<sup>6</sup>, Hiro Akinaga<sup>6</sup>

<sup>1</sup> SOLEIL Synchrotron (SOLEIL), BP48 Saint Aubain, Gif-sur-Yvette 91192, France

<sup>2</sup> Sincrotrone Trieste (ELETTRA), Basovizza (Trieste) 34012, Italy

<sup>3</sup> Arizona State University, Department of Physics and Astronomy,  
Tempe AZ 85287-1504, United States

<sup>4</sup> CNRS, Institut Néel (NEEL), 25 rue des Martyrs, Grenoble 38042, France

<sup>5</sup> CEA-Saclay, Gif-Sur-Yvette 91191, France

<sup>6</sup> National Institute of Advanced Industrial Science and Technology (AIST), Tsukuba, Ibaraki 305-8568, Japan

Email: souliman.elmoussaoui@elettra.trieste.it

Ferromagnetic MnAs is a promising candidate for electrical spin injection into GaAs and Si based semiconductors, since it exhibits a large carrier spin polarisation, small coercive field and relatively high saturation magnetisation. Bulk MnAs is ferromagnetic at RT ( $\alpha$ -phase) and shows near 40°C a second order transition to the paramagnetic  $\beta$ -phase. On contrary, epitaxial MnAs films on GaAs substrate show at RT the coexistence of both phases due to the large and anisotropic lattice mismatch. Elastic domains of both phases form a periodic stripes pattern in a self organised way [1]. The nature of the nonmagnetic phase, which coexists in thin films, is of great interest [2]. Until recently  $\beta$ -MnAs has generally been considered to be paramagnetic but first principles calculations [3] and the discovery of built-in exchange biasing suggest antiferromagnetism.

Stimulated by this controversy, we have recently re-examined our XMCD-PEEM [4], [5] results and have complemented them with corresponding linear dichroism (XMLD) studies. A temperature and an angular dependence of the XMLD signal were recently performed and the results obtained clearly evidence the antiferromagnetic nature of the beta phase. These important results end a more than 50 year old scientific controversy and allow to give a new revisited description of the magnetic behaviour in striped MnAs thin films.

### References

- [1] T. Plake et al 2002 Appl. Phys. Lett. 80, 2523
- [2] L. Däweritz 2006 Rep. Prog. Phys. 69, 2581
- [3] M. K. Niranjan, B.R. Sahu and L. Kleinman 2004 Phys. Rev. B 70, 180406
- [4] E. Bauer et al 2002 J. Vacuum Sci. Technol. B 20, 2539
- [5] L. Daeweritz et al 2005 J. Vacuum Sci. Technol. B 23, 17599

## Principles and prospects of direct high resolution electron image acquisition with CMOS detectors at low energies

A.R. Faruqi

*MRC Laboratory of Molecular Biology,  
Hills Road, Cambridge CB2 0QH, U.K.*

Email: arf@mrc-lmb.cam.ac.uk

Electron cryo-microscopy (cryo-EM) plays an important role in high resolution biological structural determination. One great advantage of cryo-EM is that it may be possible to achieve atomic resolution for large biological molecules or other macromolecular complexes without the need for crystallisation. As all biological specimen are susceptible to radiation damage, it is important to minimise the dose during data acquisition so a primary requirement is for the use of the most efficient detectors [1, 2]; to capture high resolution features detectors also need to have good spatial resolution. Both these requirements can be combined in a single property, defined as the detective quantum efficiency (DQE), and DQE as a function of spatial frequency,  $DQE(\omega)$  [3, 4]. Since detectors potentially receive large doses of radiation over their 'lifetime', it is important to design them to be sufficiently rad-hard to allow a minimum of one-year use [5].

Although film has traditionally been used for cryo-EM, and more recently phosphor fiber-optic-coupled CCDs, direct electron detection offers significant benefits over the other techniques. We discuss two types of pixel detectors in some detail, which have been developed over the past decade, viz. hybrid pixel detectors (HPDs) and monolithic active pixel sensors (MAPS) and their potential impact on electron microscopy. The sensor and readout electronics are separated in HPDs [6], which leaves open the choice of the sensor material depending on the application. On the other hand, MAPS incorporate a thin sensor and readout electronics in the same substrate [7]. Most evaluations for cryo-EM were carried out at electron energies in the range 40-300 keV. However, a number of applications require detection of electrons at much lower energies, e.g. Tritium-labelled autoradiography needs to record electrons in the range 6 – 16 keV [8]. Both type of detectors can be used at such low energies but the two important design features required are a low noise readout and a thin dead layer due to the short electron range. The passivation layer in a silicon sensor used for Medipix2 is sufficiently thin to allow low energy electrons to be recorded. For MAPS type sensors it is necessary to backthin the detectors down to the epilayer and to use them in back-illuminated geometry as described in the paper by Caballo, et al [8].

### References

- [1] A. R. Faruqi and R. Henderson, *Current Opinion in Structural Biology*, **17** (2007),549.
- [2] A. R. Faruqi, *Advances in Imaging and Electron Physics*, **145** (2007),55 – 94.
- [3] R.Henderson,G.McMullan,S.Chen and A.R.Faruqi, *Ultramicroscopy*, 2008, submitted
- [4] G. McMullan,D. M. Cattermole,S. Chen,R. Henderson,X. Llopart,C. Summerfield,L. Tlustos and A. R. Faruqi, *Ultramicroscopy*, **107** (2007),401
- [5] A. R. Faruqi,R. Henderson and J. Holmes, *Nucl Instr. and Meth.*, **565** (2006),139.
- [6] X. Llopart and M. Campbell, *Nucl. Instr. and Meth A*, **509** (2003),157.
- [7] M. L. Prydderch,N. J. Waltham,R. Turchetta,M. J. French,R. Holt,A. Marshall,D. Burt,R. Bell,P. Pool,C. Eyles and H. Mapson-Menard, *Nucl. Instr. Meth.*, **A512** (2003),358.
- [8] Jorge Cabello,Alexis Bailey,Ian Kitchen,Mark Prydderch,Andy Clark,Renato Turchetta and K. Wells, *Phys. Med. Biol.* , **52** (2007),4993–5011.

## SMART – the aberration corrected spectromicroscope with high lateral and spectral resolution

Thomas Schmidt<sup>1</sup>, Helder Marchetto<sup>1</sup>, Florian C. Maier<sup>2</sup>, Pierre L. Levesque<sup>1</sup>, Ullrich Groh<sup>2</sup>, Tomas Skala<sup>1</sup>, Helmut Kuhlbeck<sup>1</sup>, Peter Hartel<sup>3</sup>, Rainer Spehr<sup>3</sup>, Dirk Preikszas<sup>3,4</sup>, Gerhard Lilienkamp<sup>5</sup>, Rainer Fink<sup>6</sup>, Harald Rose<sup>3</sup>, Ernst Bauer<sup>5</sup>, Hans-Joachim Freund<sup>1</sup> and Eberhard Umbach<sup>2,6</sup>

<sup>1</sup>Fritz-Haber-Institut der Max-Planck-Gesellschaft, 14159 Berlin, Germany

<sup>2</sup>Universität Würzburg, Experimentelle Physik II, 97074 Würzburg, Germany

<sup>3</sup>Angewandte Physik, Technical University Darmstadt, Hochstuhlstrasse 6, D-64289 Darmstadt, Germany

<sup>4</sup>Carl Zeiss NTS GmbH, D-73447 Oberkochen, Germany

<sup>5</sup>Techn. Univ. Clausthal, Phys. Institut, D-38678 Clausthal-Zellerfeld, Germany

<sup>6</sup>Univ. Erlangen-Nürnberg, Phys. Chemie II, 91058 Erlangen, Germany

<sup>7</sup>Forschungszentrum Karlsruhe, 76021 Karlsruhe, Germany

Email: Schmidt@fhi-berlin.mpg.de

Combining high-brilliance synchrotron radiation with a parallel imaging LEEM or PEEM allows a comprehensive characterization of surfaces, adsorbates, and ultra-thin films. The SMART [1] installed at BESSY is one of the most challenging projects in this field. It aims at a lateral resolution of 2 nm, an increase in transmission by nearly two orders of magnitude and an energy resolution of 100 meV that can only be achieved by aberration correction and energy filtering, whereas the special optical layout – similar to the Bauer-type spectroscopic LEEM [2] – enables a simultaneous optimization of lateral resolution, transmission and spectral resolution. The tetrode mirror in the SMART is the first corrector [3] in an electron microscope which simultaneously compensates for both, the spherical and chromatic aberrations of the electron lens system and could already demonstrate a lateral resolution of 3.1 nm. The aberration corrected Omega-filter achieved an energy resolution of 180 meV, without affecting the lateral resolution or reducing the transmission of the system.

Utilizing different sources (linearly or circularly polarized x-rays, UV-light, electron gun, etc.) the SMART outmatches as a versatile instrument [4] with a variety of contrast mechanisms by imaging photo-emitted (XPEEM, UV-PEEM) and reflected electrons (LEEM, MEM). Thus it enables the laterally resolved study of morphology, chemical composition, electronic state, molecular orientation, magnetization, work function, structural properties, atomic steps, etc. Archetype experiments on the growth properties of organic thin films, their substrate dependence, and the internal structure of micro-crystallites of organic molecules [5] that show the potential of the instrument will be briefly presented.

Funded by the BMBF, contract 05 KS4 WWB/4.

### References

- [1] R. Fink et al., *J. Electr. Spectrosc. Rel. Phen.* **84**, 231 (1997)
- [2] Th. Schmidt, S. Heun, J. Slezak, J. Diaz, K.C. Prince, G. Lilienkamp, E. Bauer *Surf. Rev. and Lett.* **5** (1998) 1287-1296
- [3] D. Preikszas and H. Rose, *J. Electr. Micr.* **1**, 1 (1997)
- [4] Th. Schmidt et al., *Surf. Rev. Lett.* **9**, 223 (2002)
- [5] H. Marchetto, U. Groh, Th. Schmidt, R. Fink, H.-J. Freund, E. Umbach, *Chem. Phys.* **325**, 178 (2006)

## Development of Stereo-PEEM and a new display analyzer for Stereo-pictures of atomic arrangement

Hiroshi Daimon<sup>1,2</sup>, László Tóth<sup>1,2</sup>, Kentaro Goto<sup>1</sup>, Hiroyuki Matsuda<sup>1,2</sup>, and Fumihiko Matsui<sup>1,2</sup>

<sup>1</sup>Nara Institute of Science and Technology (NAIST), 8916-5 Takayama, Ikoma, Nara 630-0192, JAPAN

<sup>2</sup>CREST, Japan Science and Technology Agency, Saitama 332-0012, Japan

Email: daimon@ms.naist.jp

Stereo-PEEM [1], which is a new photoemission electron microscope (PEEM), can display not only the image of microscopic area but also the angular distribution of high-energy (more than 1 keV) photoelectrons up to about  $\pm 60^\circ$ , which is about 100-fold the acceptance angle of usual PEEM. This wide angle acceptance for high-energy photoelectrons enables the stereo-picture [2] of three-dimensional (3D) atomic arrangement as well as the 3D electronic structure [3] of individual micromaterials. The stereo-picture of 3D atomic structure of a sample can be displayed directly on the screen using circularly polarized light as an excitation source. During the project of Stereo-PEEM, high-quality stereo-pictures of atomic arrangement have been obtained, and a wide acceptance-angle electrostatic lens and a new display analyzer were invented. The present status of Stereo-PEEM, stereo-pictures and lens system for the new display analyzer are presented.

Fig. 1 shows a schematic drawing of Stereo-PEEM. Stereo-PEEM consists of a Wide Acceptance Angle (about  $1 \pi$  sr) Electrostatic Lens (WAAEL) [4], following cylindrical lenses, an energy-filter (DIANA), projector lenses and a screen with MCP. Field aperture (FA) is used to select sample regions from which the angular distribution of the emitted electrons is to be measured. This wide angular distribution of core-level photoelectrons at about 1 keV excited by circularly polarized light can be used as the stereo-photograph of atomic arrangement. A stereo-photograph of Cu crystal [5], which has been obtained by a different apparatus in SPring-8 BL25SU, is shown in the inset of Fig. 1. A new  $1 \pi$  sr Display-type Ellipsoidal Mesh Analyzer (DELMA) [6], which works as a simple PEEM and a high sensitive display-type electron energy and two-dimensional angular distribution analyzer, has also been invented using the first two parts (WAAEL and some cylindrical lenses) of Stereo-PEEM.

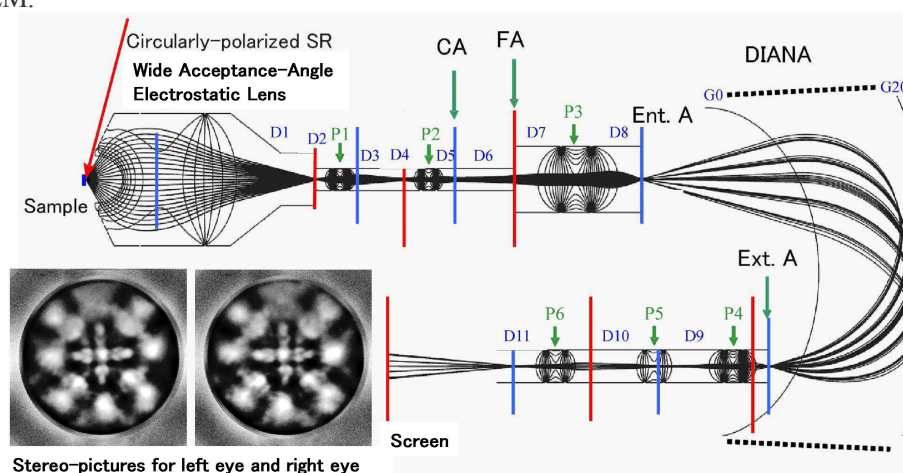


Fig. 1: schematic drawing of Stereo-PEEM

### References

- [1] H. Daimon, H. Matsuda, L. Toth, F. Matsui, *Surface Science*, 601, 20, 4748, (2007).
- [2] H. Daimon, *Phys. Rev. Lett.* 86, 2034 (2001).
- [3] H. Daimon, F. Matsui, *Progress in Surface Science*, 81, (8-9), 367, (2006).
- [4] L. Tóth, H. Matsuda, T. Shimizu, F. Matsui and H. Daimon, *J. Vac. Soc. Jpn.* 51, 135 (2008).
- [5] F. Matsui, Y. Kato, T. Matsushita, F. Z. Guo, and H. Daimon, to be submitted.
- [6] L. Tóth, H. Matsuda, T. Shimizu, F. Matsui and H. Daimon, to be submitted.



## High brightness and high polarization electron source for Spin-LEEM

T. Nakanishi<sup>1</sup>, N. Yamamoto<sup>1</sup>, A. Mano<sup>1</sup>, Y. Nakagawa<sup>1</sup>, T. Konomi<sup>1</sup>,  
M. Yamamoto<sup>1</sup>, S. Okumi<sup>1</sup>, X. Jin<sup>2</sup>, T. Ujihara<sup>2</sup>, Y. Takeda<sup>2</sup>,  
T. Ohshima<sup>3</sup>, T. Yasue<sup>4</sup>, T. Koshikawa<sup>4</sup>, T. Saka<sup>5</sup>, and T. Kato<sup>6</sup>

<sup>1</sup>Graduate School of Science, Nagoya University, Nagoya 464-8602, Japan

<sup>2</sup>Graduate School of Engineering, Nagoya University, Nagoya 464-8601, Japan

<sup>3</sup>Central Research Laboratory, Hitachi Ltd. Tokyo, 185-8601, Japan

<sup>4</sup>Fundamental Electronics Research Center, Osaka Electro-Communication University,  
Osaka 572-8530, Japan

<sup>5</sup>Daido Institute of Technology, Nagoya 457-8531, Japan

<sup>6</sup>Daido Steel Co. Ltd., Nagoya 457-8531, Japan

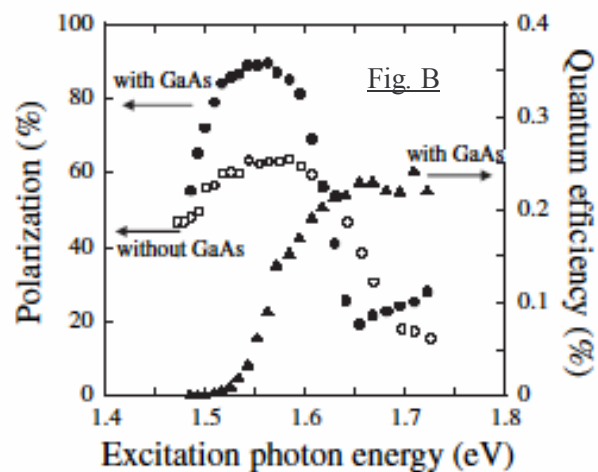
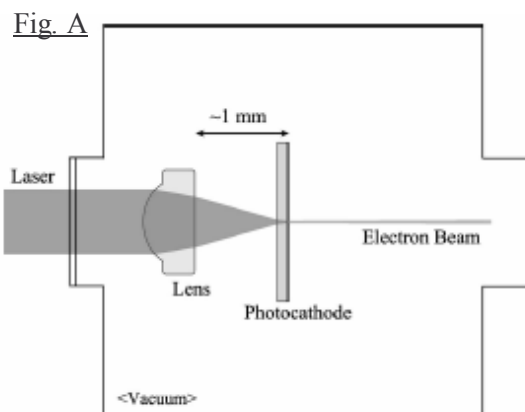
Email: nakanisi@spin.phys.nagoya-u.ac.jp

A point-like emission mechanism is required for the photocathode of a GaAs polarized electron source to produce a high brightness and high spin polarization electron beam. This is realized by changing the direction of the injection laser light from the front-side to the back-side of the photocathode as shown in Fig. A.

Based on this concept, a 20-keV gun (JPES-1) was constructed with a transmission photocathode including an active layer of a GaAs-GaAsP superlattice. This system produced a laser spot diameter as small as 1.3 $\mu$ m for the 760~810nm laser wavelength, and the brightness of  $\sim 2 \times 10^7$  A $\cdot$ cm $^{-2}$ ·sr $^{-1}$  (which corresponds to a reduced brightness of  $\sim 1.0 \times 10^7$  A $\cdot$ cm $^{-2}$ ·sr $^{-1}$ ·V $^{-1}$ ) was achieved for an extracted current of 5.3 $\mu$ A. This brightness is still smaller than those of the W-field- emitters, but one order of magnitude higher than those of LaB6 emitters [1].

The peak polarization of  $\sim 90\%$  was achieved at the same time by inserting a GaAs thin layer between the GaAsP substrate and the GaAsP buffer layer, which demonstrated that the strain-control of the GaAsP buffer layer is indispensable to achieve the highest polarization as shown in Fig. B [2]. The charge density lifetime of  $1.8 \times 10^8$  C/cm $^2$  was observed for an extracted current of  $\sim 3\mu$ A [1].

The second gun system (JPES-2) is under construction to be mounted for the LEEM apparatus operated at OECU. These works have been financially supported by Japan Science and Technology (JST) Agency as a technology development program for advanced measurements and analysis (program leader: T. Nakanishi).



### References

- [1] N. Yamamoto, T. Nakanishi et al., J. of Appl. Phys. vol.103, No. 6 (2008), 06490  
[2] X. Jin, N. Yamamoto et al., Appl. Phys. Express Vol. 1 (2008), No. 4, 045002

## Photoemission and Mirror Electron Microscopy of Ga droplets on GaAs (001)

W. X. Tang<sup>1</sup>, D. E. Jesson<sup>1</sup>, K. M. Pavlov<sup>1,2</sup>, M. J. Morgan<sup>1</sup> and B. F. Usher<sup>3</sup>

<sup>1</sup>*School of Physics, Monash University, Victoria 3800, Australia*

<sup>2</sup>*Present address: Physics & Electronics, School of Science and Technology, University of New England, NSW 2351, Australia*

<sup>3</sup>*Department of Electronic Engineering, La Trobe University, Victoria 3086, Australia*

Email: wenxin.tang@sci.monash.edu.au

GaAs (001) is one of the most intensively studied surfaces because of its importance as a prominent substrate for engineering optical and electrical devices by molecular beam epitaxy (MBE). Of particular interest is the self-assembly of quantum dots (QDs) for high modal gain lasers and applications in quantum computing and quantum cryptography. Strain induced QD self-assembly [1] has now been adopted by almost all of the groups pursuing QD device development. However, such methods are inherently limited to strained systems which severely restricts the range of dot sizes and compositions attainable. Recently, however, droplet epitaxy has been proposed as an exciting alternative approach to dot formation [2]. First, liquid Ga or In droplets are deposited on the GaAs surface. This is followed by crystallisation and subsequent transformation into QD's under As flux. The greater flexibility in composition and the capability to fabricate quantum-like structures including QD molecules, rings and double-rings offers exciting prospects for creating new structures with atom-like properties.

The emergence of droplet epitaxy as a key method of quantum structure fabrication highlights the need to understand the physics underlying Ga droplet behaviour on GaAs (001). In this paper we use mirror electron microscopy (MEM) and photoemission electron microscopy (PEEM) to study the *in situ* formation and behaviour of Ga droplets during substrate annealing. These real space studies provide unique insight into the Langmuir Evaporation of GaAs and its intimate connection to the congruent evaporation temperature. We also discuss how surface electron microscopy can be used to reconstruct droplet shape using Lloyd's Mirror PEEM [3]. This technique offers the advantage of determining droplet contact angles in real-time at elevated temperatures under deposition flux (Fig.1) providing important information on the energetics governing

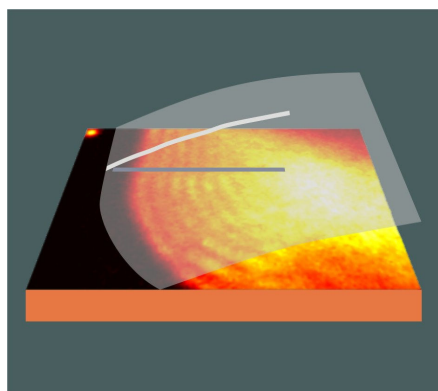


**Fig. 1.** Ga droplet surface profile (solid-line) reconstructed from the fringes in a Lloyd's Mirror PEEM image .

contact-line geometry. Atomic force and scanning electron microscopy measurements on quenched samples provide excellent agreement with the *in situ* Lloyd's Mirror PEEM data, confirming that the method can provide highly complementary 3D information.

### References

- [1] See for example, V A Shchukin and D Bimberg, *Rev. Mod. Phys.* **71**, (1995) 1125.
- [2] S. Huang *et al*, *Appl. Phys. Lett.* **89**, (2006) 031921.
- [3] D.E. Jesson, K.M. Pavlov, M.J. Morgan, and B.F. Usher, *Phys. Rev. Lett.* **99**, (2007) 016103.



## Time-of-Flight- and Spin-Filtering in Low-Energy Electron Microscopy

G. Schönhense<sup>1</sup>, P. Lushchik<sup>1</sup>, M. Hahn<sup>1</sup>, A. Krasnyuk<sup>2</sup>, A. Oelsner<sup>3</sup>, D. Panzer<sup>3</sup>, J. Kirschner<sup>2</sup>

<sup>1</sup>*Institut für Physik, Johannes Gutenberg Universität Mainz (Germany)*

<sup>2</sup>*Max-Planck-Institut für Mikrostrukturphysik, Halle (Germany)*

<sup>3</sup>*Surface Concept GmbH, Staudingerweg 7, 55128 Mainz (Germany)*

Email: schoenhense@uni-mainz.de

The manipulation of the electron beam in a low-energy electron microscope by “unconventional” insertion elements offers fascinating possibilities for the instrument performance. Besides common image information, there are additional degrees of freedom in the electron beam that can be exploited: The electrons’ time-of-flight (TOF) and spin polarisation (SP). In this contribution we will discuss novel approaches giving access to these degrees of freedom. TOF filtering is established in several groups (for a recent review see [1]), whereas spin filtering is just being tested for the first time.

**TOF-PEEM** uses the delayline detector (DLD) [2] as an imaging device, being originally developed for coincidence detection of particles. Recent advances led to a lithographically-fabricated meander-type detector that is characterised by far better impedance matching and by an excellent long-term stability compared to a wire detector containing flat coils of very thin wires around ceramics rods. In measurements on Ag dots on Si under excitation with a blue laser (400 nm) we obtained high contrast images with an ultimate dynamic range up to  $10^6$ , which surmounts the dynamic range of the common image detector (MCP-fluorescent screen-CCD camera) by orders of magnitude. This is a virtue of the coincidence technique used for image formation in a DLD, where single-electron detection is employed and the x, y and t coordinates of each counting event are determined via precise time measurements. The present time resolution of the DLD (best achieved: 108 ps) translates into an energy resolution of better than 100 meV at a drift energy below 50 eV for the given geometry of our TOF-PEEM.

The *spin degree of freedom* is exploited in SEMPA [3] (being not suited for real-time imaging of fast processes) and SP-LEEM [4] using diffraction of polarised electrons from magnetic surfaces for generating high magnetic contrast. We are developing two alternative approaches by implementing an imaging spin-filter into the column of a low-energy microscope. In the first set-up spin-polarised electron diffraction from a single crystal surface is used for spin filtering. A telescopic beam is reflected from the surface such that the electron-optical image is retained and can be further magnified and viewed on an imaging unit. A second method uses spin dependent transmission through an ultra thin ferromagnetic foil at low electron energies where the mean free path increases steeply. From spectroscopy experiments it is known that the optimum analysing power of such a transparent foil can be very high due to the differences in inelastic mean free path for low-energy electrons in ferromagnets [5]. For the generation of an electron-optical image at very low energy close to the threshold we use a special strategy that generates a magnified image on the plane of the spin filter foil.

In combination, TOF- and spin-filtering based on diffraction will constitute a spin-resolved spectromicroscope. The optimum working point of the analyser crystal allows for the simultaneous analysis of energy intervals  $> 3\text{eV}$ . In addition, dynamic refocusing of the lens system synchronised with the excitation source facilitates chromatic aberration correction.

The project is supported by DFG (SCHO 341/9-1).

### References

- [1] G.Schönhense, H.J.Elmers, S.A.Nepijko, C.M.Schneider, Adv. in Imaging and El. Phys. **142**, 159 (2006)
- [2] A. Oelsner et al., Rev. Sci. Instrum. **72**, 3968 (2001)
- [3] H.P. Oepen, J. Kirschner, Scanning Microsc. **5**, 1 (1991)
- [4] Th. Duden, E. Bauer, Surf. Rev. Lett. **5**, 1213 (1998)
- [5] G. Schönhense, H. C. Siegmann, Ann. Phys. **2**, 465 (1993)

## LEEM and PEEM: Past and Future

Ernst Bauer

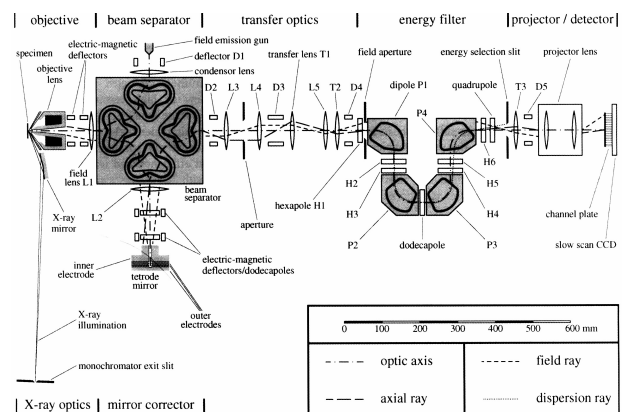
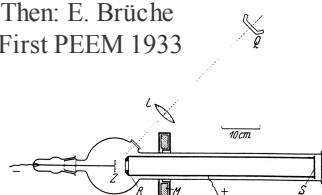
Department of Physics

Arizona State University, Tempe, Arizona 85287-1504, USA

Email: ernst.bauer@asu.edu

In this talk I will try to sketch the evolution of PEEM and LEEM over the 75 years since the first PEEM images were published [1]. From the primitive instruments of the early 30ies the understanding and instrumentation developed rapidly until the early 40ties when the war and its aftermath delayed further work. The 50ies saw a renaissance of emission and other cathode lens microscopy development and research until in the early 60ties metal UHV became available and LEEM was invented [2]. From thereon the field developed slowly until combined LEEM-PEEM instruments became commercially available in the mid-90ties. The addition of energy resolution, the development of aberration correction and of various experimental methods such as magnetic circular dichroism PEEM and pump-probe techniques, finally brought the field to the present state of sophistication. The history of the field has been described in several reviews [3-6]. A few milestones are the famous Recknagel formula for the resolution limit of emission microscopes [7] which was long inappropriately also used against LEEM, Engel's emission microscope that reached today's resolution 40 years ago [8] and Teliép's LEEM study of the Si(111) (1x1)-(7x7) phase transition [9], which put finally LEEM onto the scientific map.

Then: E. Brüche  
First PEEM 1933



Now: H. Rose, D. Preikszas, First aberration-corrected instrument 1995 ...200x

With all the advances in instrumentation and techniques made in recent years by an increasing number of players and the developments presently in progress, the future of cathode lens electron microscopy looks bright. Aberration correction not only will move the resolution into the nm range but, more importantly, will increase the transmission considerably, new light sources and new detectors will allow widespread in-house spectromicroscopy and new techniques such as time-of-flight and multi-photon excitation will open up new application fields, to mention only a few promises of the future.

### References

- [1] E. Brüche, *Z. Phys.* **86**, 448 (1933).
- [2] E. Bauer, in *5<sup>th</sup> Intern. Congr. Electron Microscopy* (Academic Press, 1962), D11.
- [3] G. Möllenstedt and F. Lenz, *Adv. Electronics Electron Phys.* **18**, 251 (1963)
- [4] R.A. Schwarzer, *Microscopica Acta* **84**, 51 (1981)
- [5] O.H. Griffith and W. Engel, *Ultramicroscopy* **36**, 1 (1991)
- [6] E. Bauer, *Surf. Sci.* **299/300**, 102 (1994)
- [7] A. Recknagel, *Z.Phys.* **120**, 333 (1943)
- [8] W. Engel, *Ph.D. Thesis* (Freie Universität Berlin, 1968)
- [9] W. Teliéps and E. Bauer, *Surf. Sci.* **162**, 163 (1985)

## Evidence of Anomalous Diffusion of Pb on Si(111) from LEEM observations of Non-Equilibrium Profile Evolution

K.L. Man<sup>1</sup>, M.M.T. Loy<sup>1</sup>, M.C. Tringides<sup>2</sup>, M.S. Altman<sup>1</sup>

<sup>1</sup>*Department of Physics, Hong Kong University of Science and Technology  
Clear Water Bay, Kowloon, Hong Kong, China*

<sup>2</sup>*Department of Physics and Astronomy, Iowa State University, Ames, Iowa, U.S.A.*

Email: phaltman@ust.hk

The growth of uniform height Pb quantum islands on the Si(111) surface exhibits several novel phenomena, particularly rapid self-organization of island height at low temperature ( $150\text{K} < T < 240\text{K}$ ) [1-3]. Although quantum well states that are caused by electron confinement are known to drive the height selection, the origins of the remarkable island growth kinetics and other unusual growth behavior are less well understood. The possibility that these phenomena point to exceptionally fast Pb mass transport has stimulated interest in surface diffusion of the dense Pb wetting layer out of which Pb islands grow [3]. In the present work, we have used low energy electron microscopy (LEEM) to study surface diffusion directly. This is done by observing the temporal evolution of non-equilibrium coverage profiles that are prepared by laser induced thermal desorption (LITD). Real-time LEEM observations of profile evolution towards equilibrium uniform coverage distribution reveal several surprising features. First, the initial coverage step profile that is produced by LITD is observed to propagate from the edge of the desorption region at approximately constant velocity and with largely unperturbed step profile shape (Fig. 1a-d). This is in stark contrast to the characteristic profile broadening that is predicted by the diffusion equation, as exhibited in CO/Pt(111) profile evolution (Fig. 1e-h). Equilibration in Pb/Si(111) also occurs unusually fast, in particular, about fifty times faster than in CO/Pt(111) at 300K and disproportionately faster at lower temperature. However, rapid profile advance is attenuated sharply if the amount of Pb that is initially present in the wetting layer is even slightly less than the critical coverage  $\theta_c = 1.31$  ML. A model in which mass transport is mediated by fast adatom diffusion on top of the wetting layer subject to adatom-vacancy pair creation and annihilation will be discussed as one possible explanation of the observed profile evolution behavior. Alternatively, these observations may suggest an even more intriguing type of surface diffusion that has not been observed before.

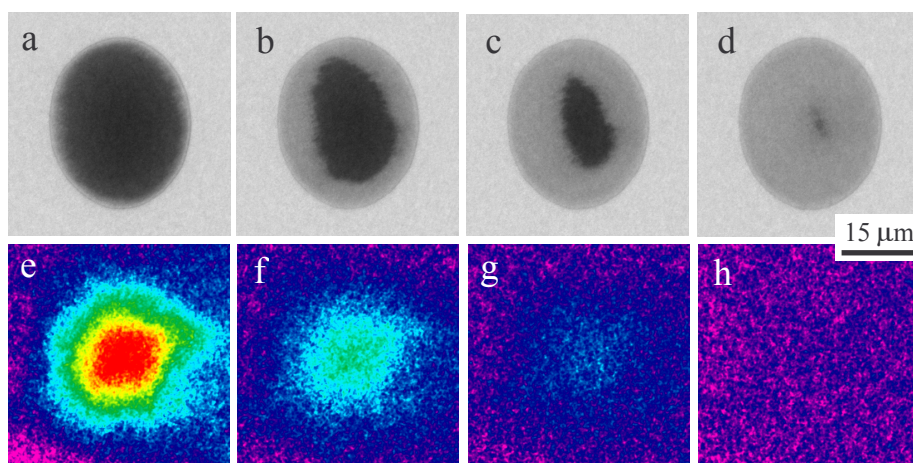


**Figure 1.** LEEM images of non-equilibrium coverage profile evolution at 300 K in (a)-(d) Pb/Si(111) and (e)-(h) CO/Pt(111). The times after (a) are (b) 0.6 sec, (c) 1.2 sec, (d) 2.0 sec. The times after (e) are (f) 27.5 sec, (g) 55 sec, (h) 110 sec.

### References

- [1] K. Budde, E. Abram, V. Yeh and M.C. Tringides, *Phys. Rev. B* **61**, R10602 (2000).
- [2] H. Hong *et al.*, *Phys. Rev. Lett.* **90**, 076104 (2003).
- [3] M. Hupalo and M.C. Tringides, *Phys. Rev. B* **75**, 235443 (2007).

## LEEM and LEEM-IV investigations of Pd/Cu(001) surface alloys: surface diffusion, Pd dissolution, and island buckling

E. Bussmann<sup>1</sup>, J. B. Hannon<sup>2</sup>, J. Sun<sup>3</sup>, K. Pohl<sup>3</sup>, and G. L. Kellogg<sup>1</sup>

<sup>1</sup>*Sandia National Laboratories\*, Albuquerque, NM 87187, USA*

<sup>2</sup>*IBM Research Division, T. J. Watson Research Center, Yorktown Heights, New York 10598, USA*

<sup>3</sup>*Department of Physics, University of New Hampshire, Durham, New Hampshire 03824, USA*

Email: glkello@sandia.gov

Ultra-thin films of Pd on Cu(001) are of interest not only as model systems for metal-metal surface alloy formation, but also as potential electromigration inhibitors for Cu interconnect applications [1]. To determine how alloyed Pd affects Cu surface self-diffusion, we are studying the decay of 2-D islands as a function of temperature and Pd concentration. These studies are made possible by previous investigations, in which we determined the distribution of Pd in the top three Cu layers from multiple-scattering-theory fits to LEEM-IV spectra [2]. Here, we use LEEM-IV spectra in a “fingerprinting” mode to monitor the Pd concentration during deposition and island decay. Measurements of decay rates as a function of temperature show that the activation energy for island decay increases from  $0.82 \pm 0.04$  to  $0.99 \pm 0.06$  eV when 0.06 ML of Pd is alloyed into the second layer. Experiments at higher coverages are complicated by the fact that Pd is lost from the second layer at higher temperatures. We are investigating the mechanism of this Pd dissolution, which appears to involve Pd moving laterally into nearby step bunches. In separate experiments, we are investigating the possibility of using LEEM-IV to measure variations in interlayer spacing across Pd/Cu alloy islands, for both islands incorporated into the top Cu layer and islands on top of the surface. Preliminary results indicate that it is possible to extract the spatial variation in concentration and interlayer spacing separately from the LEEM-IV analysis.

\*Work performed at Sandia was supported by the U.S. DOE, Office of BES, DMSE. Sandia is operated by Sandia Corporation, a Lockheed Martin Company, for the U. S. DOE’s NNSA under Contract No. DE-AC04-94AL85000. Work at UNH was supported by the NSF under Grant No. DMR-0134933.

### References

[1] C. K. Hu, et al., Appl. Phys. Lett. 81, 1782 (2002).

[2] J. B. Hannon, J. Sun, K. Pohl and G. L. Kellogg. Phys. Rev. Lett. 96, 246103 (2006).



## Labyrinth-like island growth during Pd/Ru(0001) heteroepitaxy.

N. Rougemaille<sup>1,2,3</sup>, F. El Gabaly<sup>2,4</sup>, R. Stumpf<sup>3</sup>, A. K. Schmid<sup>2</sup>, K. Thürmer<sup>3</sup>, N.C. Bartelt<sup>3</sup>, and J. de la Figuera<sup>4</sup>

<sup>1</sup> Institut Néel, CNRS & Université Joseph Fourier, BP166, F-38042 Grenoble cedex 9, France

<sup>2</sup> NCEM, Lawrence Berkeley National Laboratory, Berkeley, California 94720, USA

<sup>3</sup> Sandia National Laboratories, Livermore, California 94550, USA

<sup>4</sup> CMAM, Universidad Autónoma de Madrid, Madrid 28049, Spain

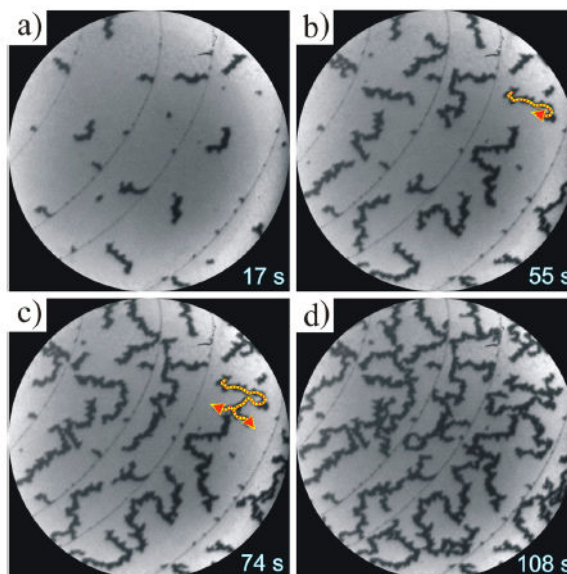
Email: akschmid@lbl.gov

While depositing atomic palladium layers on Ru(0001) surfaces, LEEM observations reveal an unusual epitaxial growth mode. After an initial stage where Pd starts to decorate the Ru step edges, the growth continues only from a few separated locations. As more Pd is deposited on the Ru surface, the growth proceeds by forming snake-like islands [1].

This growth mode is puzzling because at sufficiently high temperature, epitaxial growth commonly occurs by the flow of atomic steps: atoms deposited on terraces on the surface of a crystal diffuse across that surface until they encounter steps. At steps, the atoms are incorporated, causing the steps to advance. This is clearly not the case here, where a striking 100 nm length-scale patterned growth mode is found.

Moreover, in usual cases of epitaxial growth, growing islands are easily able to coalesce. In the present case of Pd/Ru, we observe instead that the islands *avoid* connecting with other islands or with the substrate steps. When advancing step regions come close to other, immobile step segments, they turn away, and often split in two. This process gives rise to labyrinth patterns.

The figure shows LEEM images of the Pd growth process on Ru(0001) at 840 K. Field of view is 6 micron. After first uniformly decorating the step edges in (a), the Pd grows only from several distinct locations. In (b) and (c) the self-avoiding nature of different growth fronts is evident: Colliding growth fronts turn aside or split rather than coalesce.



To understand the atomic mechanisms that cause this growth behavior, we compare scanning tunneling microscopy and LEEM experiments with results from density functional theory and Monte Carlo simulations. We find that a surface alloy forms around the growing islands. We propose that this surface alloy gradually reduces step attachment rates, which results in an instability that favors adatom attachment at fast advancing step sections.

### References

[1] N. Rougemaille, F. El Gabaly, R. Stumpf, A. K. Schmid, K. Thürmer, N. C. Bartelt, and J. de la Figuera, Phys. Rev. Lett. **99** 106101 (2007).

## Using LEEM-based electron reflectivity to understand how graphene grows on ruthenium

Kevin F. McCarty, Elena Loginova, and Norman C. Bartelt  
*Sandia National Laboratories, Livermore, California 94550, USA*

Email: [mccarty@sandia.gov](mailto:mccarty@sandia.gov)

Understanding and controlling film growth has long been a key focus of the surface-science and technology communities. The growth physics of many simple metals, semiconductors, and even large organic molecules are well understood. In contrast, the detailed growth physics of graphitic carbon films has not been elucidated. This is particularly true for graphene, which is a single atomic sheet of graphitic carbon arranged in a honeycomb crystal lattice. Currently there is an intense, worldwide effort researching the exotic electronic properties of graphene. Furthermore, graphene is widely used in the rapidly developing field of carbon nanoscience. Despite the large efforts in growing large and defect-free graphene crystals, many basic questions remain unanswered. In particular, graphene's growth species and the factors that control the nucleation and growth rates are not known.

We have used LEEM to simultaneously measure: 1) the instantaneous growth rate of individual graphene islands on Ru(0001) and 2) the local concentration of mobile carbon atoms from which the graphene grows. The latter is measured from changes in electron reflectivity [1], which we find to be precisely proportional to the carbon adatom concentration. By calibrating with known coverages, we are able to measure the absolute carbon adatom concentration. By measuring the local change in electron reflectivity from the brightness of LEEM images, the local carbon atom concentration is determined, for example, next to a growing graphene island.

The behavior of graphene growth we observe is very striking and in sharp contrast to metal epitaxy. We find that a large barrier exists for carbon monomers to attach to graphene step edges: 1) graphene edge motion is limited by C atom attachment and not by C atom diffusion. 2) The absolute value of the supersaturation required for appreciable growth rates is comparable to supersaturation required to nucleate new islands. 3) The growth rate as a function of supersaturation is highly nonlinear, with a surprisingly large activation energy. We will discuss a model that explains all these observations and gives large insights into the molecular processes by which graphene grows. Using this knowledge and method, we will show how the nucleation density and location can be precisely controlled. Finally, we will discuss the generality and physical origins of the electron reflectivity method.

This research was supported by the Office of Basic Energy Sciences, Division of Materials Sciences, U. S. Department of Energy under Contract No. DE-AC04-94AL85000.

### References

[1] J. de la Figuera, N. C. Bartelt, and K. F. McCarty, *Surface Science*, **600** 4062 (2006).

## Step Structure and Motion on an icosahedral-AIPdMn Quasicrystal

Y. Sato<sup>1,2</sup>, B. Unal<sup>3,5</sup>, K.F. McCarty<sup>6</sup>, N.C. Bartelt<sup>6</sup>, A.K. Schmid<sup>2</sup>, T. Duden<sup>2</sup>,  
K. Pussi<sup>7</sup>, T.A. Lograsso<sup>5</sup>, C.J.Jenks<sup>5</sup>, P.A. Thiel<sup>3,4,5</sup>

<sup>1</sup>*Department of Physics, University of California, Davis, California, U.S.A.*

<sup>2</sup>*National Center for Electron Microscopy, Lawrence Berkeley National Laboratory,  
Berkeley California, U.S.A.*

<sup>3</sup>*Department of Materials Science and Engineering, Iowa State University, Ames, Iowa, U.S.A*

<sup>4</sup>*Department of Chemistry, Iowa State University, Ames, Iowa, U.S.A*

<sup>5</sup>*Ames Laboratory, Ames, Iowa, U.S.A.*

<sup>6</sup>*Sandia National Laboratories, Livermore, California, U.S.A.*

<sup>7</sup>*Department of Electrical Engineering, Lappeenranta University of Technology, Finland*

Email: yusato@ucdavis.edu

We have used LEEM and STM to characterize step structure and motion on a well-ordered, aperiodic icosahedral-AIPdMn quasicrystal surface. Real-time imaging capability of LEEM allows us to understand how the room temperature quasicrystal surface develops following high temperature annealing up to 910K. The way steps move on this surface at high temperature is remarkable. Two types of steps move with different velocities and cross each other. What is more, the two steps form a chicken wire-like hexagonal and rhombohedral mesh structure, as the steady-state surface morphology [Figure(a)]. From the STM step height measurement, the two steps are identified to be L and (L+M) steps, with different step heights. ( L(6.8Å) and M(4.2Å) steps are two steps known to occur on this surface[1]).

When the surface is cooled, extensive mass flow from the surface into the bulk has large consequences upon the step motion dynamics and resultant step structure at room temperature. M steps hidden in the step crossings of chicken wire step-networks open up and extend, as it allows a new surface layer to be exposed, and thereby forming the brick-like step structure observed at room temperature, composed of L, M, and (L+M) steps [Figure(b)].

An obvious question is how one might understand the presence of periodic step arrays at the surface of quasicrystalline samples. One would expect the stacking of the two step heights to follow the Fibonacci sequence of the bulk quasiperiodic order [1 and references therein]. By permitting localized regions of the surface where the topmost plane trades position with the near-surface plane directly underneath, we propose a construction scheme that allows a step network consistent with experimental observations. Specific planar defects observed in icosahedral AIPdMn could enable such mechanism [2]. We discuss possible ways for this "carpet" of surface layers to be connected with the underlying bulk aperiodicity.

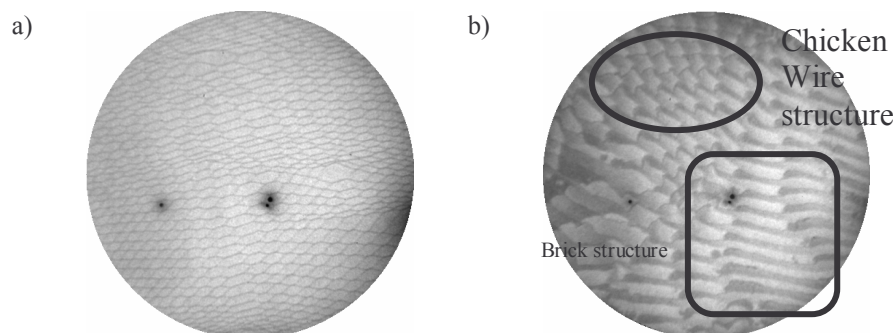


**Figure.** Bright-field LEEM images (7 $\mu$ mFOV) of a) high temperature quasicrystal surface at 905K, at electron energy of 4.4eV showing “chicken wire” array of surface steps. b) room temperature quasicrystal surface, showing both chicken wire and brick step structure.

### References

- [1] T.M. Schaub, D.E. Beurgler, and H.-J. Guntherodt, 1994 *Phys.Rev.Lett.* 73, 1255  
[2] M. Feuerbacher, M. Heggen, and K. Urban, 2004 *Mat.Sci.and Eng. A* 375-377, 84

## Magnetization Dynamics of Magnetic Microstructures Using Time-Resolved PEEM with Deflection Gating

Alexander Kaiser, Carsten Wiemann, Stefan Cramm, Claus M. Schneider  
*Forschungszentrum Jülich, Institut für Festkörperforschung IFF-9, Jülich, Germany*

Email: a.kaiser@fz-juelich.de

Time-resolved photoelectron emission microscopy (TR-PEEM) using synchrotron radiation is a well-known method for studying element-resolved magnetization dynamics with a stroboscopic approach [1]. The drawback of this method is the dependence on the time structure of the probing beam since the repetition frequency of the magnetic field pulse must be an integer multiple of the probing beam frequency. In order to become independent of the BESSY-II pulse scheme we have developed an approach of switching the photoelectron beam in the microscope by a system of pulsed deflector plates. The unwanted photoelectrons are deflected away from the optical axis and are blocked by the contrast aperture (see Fig. 1 (a)). By this method we have been able to successfully use the hybrid bunch in the BESSY-II multi bunch pattern (Fig. 1 (b)) for imaging magnetization dynamics in different types of samples. Fig 1 (c) shows one XMCD image with the magnetization pattern of a  $10 \times 10 \mu\text{m}$  Iron structure, which was imaged with the gating technique.

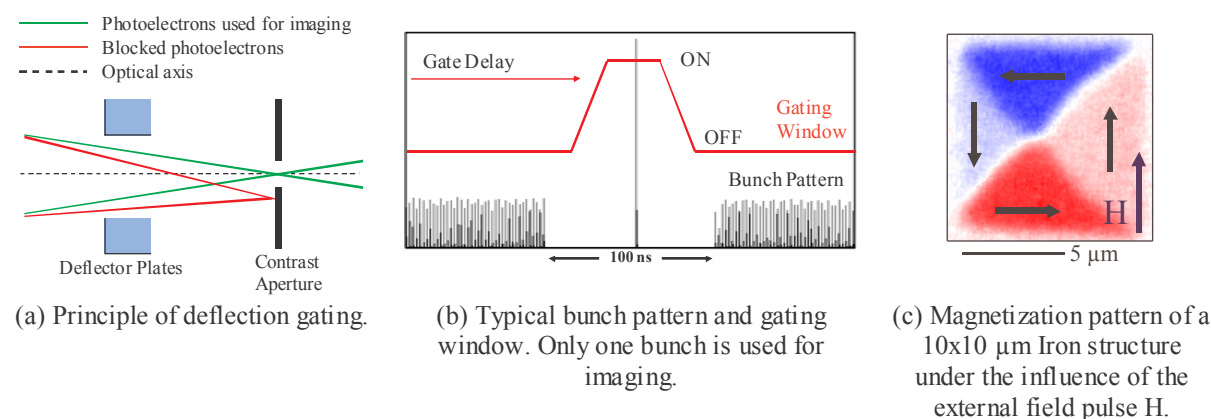


**Figure 1**

In our setup the magnetic excitation pulses are generated by an electronic high-frequency pulse generator which is connected to a coplanar waveguide lithographically defined on the samples by optical lithography. On this coplanar waveguide magnetic structures of different sizes in the micrometer regime have been microstructured. The micromagnetic response of such structures on the magnetic excitation is investigated with the above specified time-resolved setup.

We have studied several types of magnetic systems, including polycrystalline Permalloy films, epitaxially grown Iron films and interlayer-coupled trilayer systems consisting of different magnetic materials. The results of the time-resolved measurements on the different types of samples are presented and discussed in terms of different sample properties due to magneto-crystalline anisotropy and interlayer coupling.

### References

[1] Schönhense, Elmers, Nepijko, Schneider, *Adv. Im. El. Phys.* 142, 159 (2006).



## Field dependence of the vortex core speed in micron-sized FeNi disks

Keiki Fukumoto<sup>1</sup>, Kuniaki Arai<sup>2</sup>, Tomohiro Matsushita<sup>1</sup>, Hitoshi Osawa<sup>1</sup>, Tetsuya Nakamura<sup>1</sup>, Takayuki Muro<sup>1</sup>, Takashi Kimura<sup>2,3</sup>, Yoshichika Otani<sup>2,3</sup>, and Toyohiko Kinoshita<sup>1,4</sup>

<sup>1</sup>Spring-8/JASRI, 1-1-1 Kouto, Sayo, Sayo, Hyogo 679-5198, Japan

<sup>2</sup>ISSP, University of Tokyo, 5-1-5Kashiwanoha, Kashiwa, Chiba 277-8581, Japan

<sup>3</sup>RIKEN FRS, 2-1 Hirosawa, Wako, Saitama 351-0198, Japan

<sup>4</sup>CREST, Japan Science and Technology Agency, Honcho 4-1-8, Kawaguchi 332-0012, Japan

Email: keiki@spring8.or.jp

Investigating the ultrafast dynamical properties in micron-sized magnetic particles is now one of the issues for the application to spintronic devices. Here we investigated the motion of magnetic vortex in a disk-shaped Fe<sub>20</sub>Ni<sub>80</sub> element ( $\phi=6\ \mu\text{m}$ ) with response to the magnetic field strength by means of time-resolved XMCD-PEEM using a pump-probe technique. The pump was a 300 picosecond-long in-plane external field created from the electric current passing through a strip-line ( $I_{\text{strip-line}}$ ) excited by a femtosecond laser pulse. The repetition rate was 3 MHz. The pump field pushed the vortex core towards perpendicular to the field direction, and the speed of the core during the field pulse is measured for several field amplitudes, i.e.,  $I_{\text{strip-line}}$ , (see Figure). The speed increased up to 4000 m/s and saturated. This maximum speed is larger than the speed of a one-dimensional magnetic domain wall obtained in Ref. [1] and [2], and this may arise from the difference of the magnetic energy between a wall and a core. After the core displaced near the edge of the disk the core showed a one-axial oscillatory motion about the disk center with the frequency of around 50 MHz which is consistent with the result in Ref. [3] and [4], by considering the disk aspect ratio (thickness/radius=0.013).

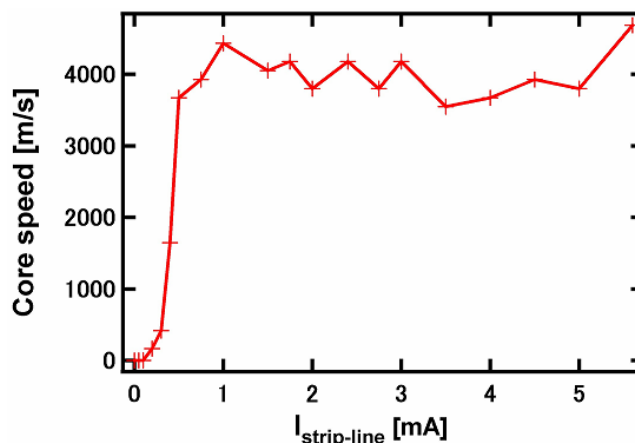


**Figure.** The core speed vs. DC current of the strip-line ( $I_{\text{strip-line}}$ ). The core speed increased up to 4000 m/s and saturated.

### References

- [1] Y. Nakatani *et al.*, Nature Materials 2 (2003) 521.
- [2] K. Fukumoto *et al.*, Phys. Rev. Lett., 96 (2006) 097204.
- [3] K. Yu. Guslienko *et al.*, Phys. Rev. Lett., 96 (2006) 067205.
- [4] J. Shibata *et al.*, J. Magn. Magn. Mat., 310 (2007) 2041.

## Magnetic Dichroism of Magnetic Ultrathin Films using Laser -PEEM

Takeshi Nakagawa, Toshihiko Yokoyama  
*Institute for Molecular Science*

Email: nakagawa@ims.ac.jp

Magnetic circular dichroism with synchrotron radiation has been an inevitable tool for the investigation of magnetic thin films, and its application for PEEM finds element specific magnetic domain imaging. Its strong contrast is due to the strong spin orbit coupling in core level and large spin polarization in valence level. On the contrary, the magnetic domain imaging in lab using PEEM is very limited [1] because laser and lamp in laboratories usually excite valence electrons, whose spin orbit coupling is weak. However angle resolved photoemission studies of magnetic thin films showed more than 10 % asymmetry of magnetic circular dichroism [2,3]. This large dichroism can be due to the energy and angle resolve experiment, and the integration of photoelectrons over the angle and energy will decrease the asymmetry. We have shown that the asymmetry becomes large only near the photoemission threshold because of its limitation of electron energy and momentum [4].

Using this finding, we have observed MCD-PEEM [5]. The magnetic contrast (several % or more) is large enough to be measured in PEEM in a short accumulation time (<1 min). Figure shows magnetic domain imaging by MCD PEEM. The sample is a perpendicularly magnetized Cs/Ni(12 ML)/Cu(001). The sample's workfunction is changed using Cs deposition near the laser energy used (~3.2 eV) to make the asymmetry large.

Two-photon photoemission experiment using short pulse laser also gives MCD contrast, and we will show results for two-photon MCD [6]. We will demonstrate that pulse laser make it possible to perform a time resolved experiment with 1 ps resolution.



**Figure.** MCD-PEEM image on Cs/Ni(12 ML)/Cu(001). The excitation source is second harmonics (3.1 eV) of Ti:Sapphire laser. The two domains correspond to up and down magnetization domains.

### References

- [1] G.K.L. Markx, H.J. Elmers, and G. Schoenhense, 2000 *Phys. Rev. Lett.*, 84, 5888.
- [2] C. M. Schneider, *et al.*, 1991 *Phys. Rev. B*44, R12066.
- [3] W. Kuch and C.M. Schneider, 2001 *Rep. Prog. Phys.*, 64, 147.
- [4] T. Nakagawa, and T. Yokoyama, 2006 *Phys. Rev. Lett.* 96, 237402.
- [5] T. Nakagawa, T. Yokoyama, M. Hosaka, and M. Katoh, 2007 *Rev. Sci. Instrum.*, 78 023907.
- [6] T. Nakagawa, *et al.*, To be published.

## Surface Plasmon Polariton Microscopy

N. Raß<sup>1</sup>, N.M. Buckanie<sup>1</sup>, L.I. Chelaru<sup>1,2</sup>, C. Wirtz<sup>1</sup>, F.-J. Meyer zu Heringdorf<sup>1</sup>

<sup>1</sup>Universität Duisburg-Essen, FB Physik and Center for Nanointegration (CeNIDE), Lotharstrasse 1, 47057 Duisburg, Germany

<sup>2</sup>present address: FZ Jülich, Institute of Solid State Research, 52425 Jülich, Germany

Email: meyerzh@uni-due.de

The interaction of frequency doubled femtosecond laser pulses with Ag nanostructures provides a fantastic playground to study surface plasmon polariton (SPP) phenomena in such structures. After frequency doubling of the fundamental fs laser pulses – provided by a commercial Ti:Sapphire oscillator with sub 20fs pulse duration – the photon energy of the  $\lambda=400$  nm laser pulses matches the plasmon resonance of the Ag particles very well. Accordingly, SPP waves can be easily excited at the edge of Ag islands.

In two photon photoemission PEEM, SPPs are imaged as a superposition of the electric field of the travelling SPP wave with the electric field of the laser pulse that hits the surface under grazing incidence. As the SPP and the fs laser pulse travel at different speeds, a beat pattern is formed across the island that can be directly imaged in PEEM (see Figure). The period of the beat pattern depends on several factors. First, the period is influenced by the angle between the propagation direction  $k_p$  of the SPP wave and the projection of the direction of incidence of the laser pulse into the surface plane  $k_{ip}$ . Second, the wavelength of the SPP wave has a dramatic effect on the period of the beat pattern: A change of the SPP wavelength by only 1 nm – which can for instance be achieved by deposition of C60 on top of the Ag island – changes the beat pattern period by 60nm, easily detectable in PEEM.

The superposition of the fs laser pulse and the SPP also influences the optical near-field behind the island: As is easily visible in the figure, a periodic undulation of maxima and minima is observed behind the island as well. Surprisingly, this pattern is correlated with the beat pattern that is observed on the particle. In a pump-probe experiment, where two coherent fs laser pulses are mutually time-delayed, it is possible to observe the propagation of the SPP, to shift the beat pattern across the island, and to control the location of maximum intensity behind the particle. Our new home-built and actively stabilized interferometer provides us with pump- and a probe pulse with attosecond accuracy. On this timescale, properties of the SPP propagation can be directly mapped in time and space.

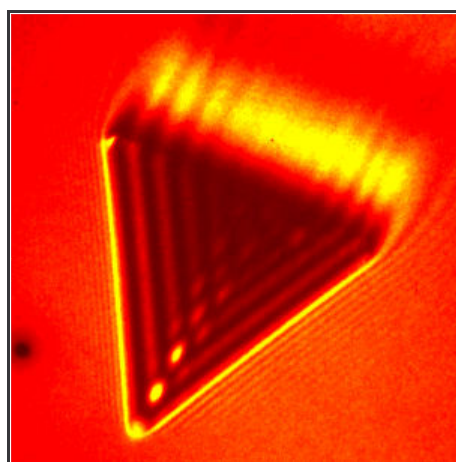


**Figure.** Triangular Ag island on a Si(111) surface in two-photon photoemission PEEM. The fs laser pulses come from the lower left and hit the surface plane under an incidence angle of  $\sim 15^\circ$ . A pronounced beat pattern is visible, caused by the superposition of two traveling SPP wave with the fs laser pulses. Behind the island, the intensity distribution is also determined by the superposition. The field of view is  $30\mu\text{m}$ .

## **Ferroelectric, Ferromagnetic, and Multiferroic Oxide Thin Films: Basic Physics, Emerging Applications, and their Growth by MBE**

Darrell G. Schlom

*Department of Materials Science and Engineering, Cornell University, U.S.A.*

Schlom@Cornell.edu

The broad spectrum of electronic and optical properties exhibited by oxides offers tremendous opportunities for microelectronic devices, especially when a combination of properties in a single device is desired. Here I describe the use of reactive molecular-beam epitaxy (MBE) to synthesize functional oxides, including ferroelectrics, ferromagnets, and materials that are both at the same time. Due to the dependence of properties on direction, it is often optimal to grow functional oxides in a particular direction to maximize their properties for a specific application. But thin film techniques offer more than orientation control; customization of the film structure down to the atomic-layer level is possible. Numerous examples of the controlled epitaxial growth of oxides, including superlattices and metastable phases, are shown. In addition to integrating functional oxides with conventional semiconductors [1], standard semiconductor practices involving epitaxial strain [2,3], confined thickness [4], and modulation doping can also be applied to functional oxide thin films [5]. Results of fundamental scientific importance as well as results revealing the tremendous potential of utilizing functional oxide thin films to create devices with enhanced performance are described.

### **References**

- [1] A. Schmehl, V. Vaithyanathan, A. Herrnberger, S. Thiel, C. Richter, M. Liberati, T. Heeg, M. Röckerath, L. Fitting Kourkoutis, S. Mühlbauer, P. Böni, D.A. Muller, Y. Barash, J. Schubert, Y. Idzerda, J. Mannhart, and D.G. Schlom, "Epitaxial Integration of the Highly Spin-Polarized Ferromagnetic Semiconductor EuO with Silicon and GaN," *Nature Materials* **6** (2007) 882-887.
- [2] J.H. Haeni, P. Irvin, W. Chang, R. Uecker, P. Reiche, Y.L. Li, S. Choudhury, W. Tian, M.E. Hawley, B. Craigo, A.K. Tagantsev, X.Q. Pan, S.K. Streiffer, L.Q. Chen, S.W. Kirchoefer, J. Levy, and D.G. Schlom, "Room-Temperature Ferroelectricity in Strained SrTiO<sub>3</sub>," *Nature* **430** (2004) 758-761.
- [3] K.J. Choi, M.D. Biegalski, Y.L. Li, A. Sharan, J. Schubert, R. Uecker, P. Reiche, Y.B. Chen, X.Q. Pan, V. Gopalan, L.-Q. Chen, D.G. Schlom, and C.B. Eom, "Enhancement of Ferroelectricity in Strained BaTiO<sub>3</sub> Thin Films," *Science* **306** (2004) 1005-1009.
- [4] D.A. Tenne, A. Bruchhausen, N.D. Lanzillotti-Kimura, A. Fainstein, R.S. Katiyar, A. Cantarero, A. Soukiassian, V. Vaithyanathan, J.H. Haeni, W. Tian, D.G. Schlom, K.J. Choi, D.M. Kim, C.B. Eom, H.P. Sun, X.Q. Pan, Y.L. Li, L.Q. Chen, Q.X. Jia, S.M. Nakhmanson, K.M. Rabe, and X.X. Xi, "Probing Nanoscale Ferroelectricity by Ultraviolet Raman Spectroscopy," *Science* **313** (2006) 1614-1616.
- [5] D.G. Schlom, L.Q. Chen, X.Q. Pan, A. Schmehl, and M.A. Zurbuchen, "A Thin Film Approach to Engineering Functionality into Oxides," *Journal of the American Ceramic Society* (August, 2008 issue).

## Imaging ferroelectric domains using low energy electrons

Salia Cherifi

*Institut Néel, CNRS & UJF, 25, rue des Martyrs, F-38042 Grenoble, France*

Email: [salia.cherifi@grenoble.cnrs.fr](mailto:salia.cherifi@grenoble.cnrs.fr)

Magnetic multiferroic materials simultaneously show ferroelectricity and ferro- or antiferromagnetism. The interaction between the magnetization and the dielectric polarization is called magnetoelectric coupling. This effect makes multiferroics particularly appealing for applications and might yield to new concept of devices such as electric field-controlled magnetic data storage or magnetic field-controlled ferroelectric memories. However, two major technical hitches retard the development of single phase multiferroics in spintronic devices: first, only a very small fraction of the existing single phase multiferroics shows robust electric and magnetic polarizations at room temperature; second, the study of the fundamental properties of multiferroic materials requires the use of a sophisticated analysis techniques and multi-method instruments.

We have recently demonstrated the possibility of imaging ferroelectric domains with low velocity electrons using the Elmitec LEEM microscope at Elettra. In this study, “up” and “down” -polarized ferroelectric nano-strips have been designed on thin multiferroic films by applying local electric fields through a conducting tip in a piezoelectric force microscope (PFM). The LEEM observation of the same regions show periodic bright and dark strips that can be clearly matched to the ferroelectric domains imaged with PFM (cf. Fig). Atomic force microscopy measurements performed prior and after the LEEM experiment exclude the contribution of topography to this striped contrast and confirm the possibility of imaging ferroelectric domains using LEEM.

This high-resolution direct imaging method of ferroelectric domains is expected to open new possibilities for the study of the domain and domain walls propagation dynamics in multiferroics, in particular when combined with XMC(L)D-PEEM.

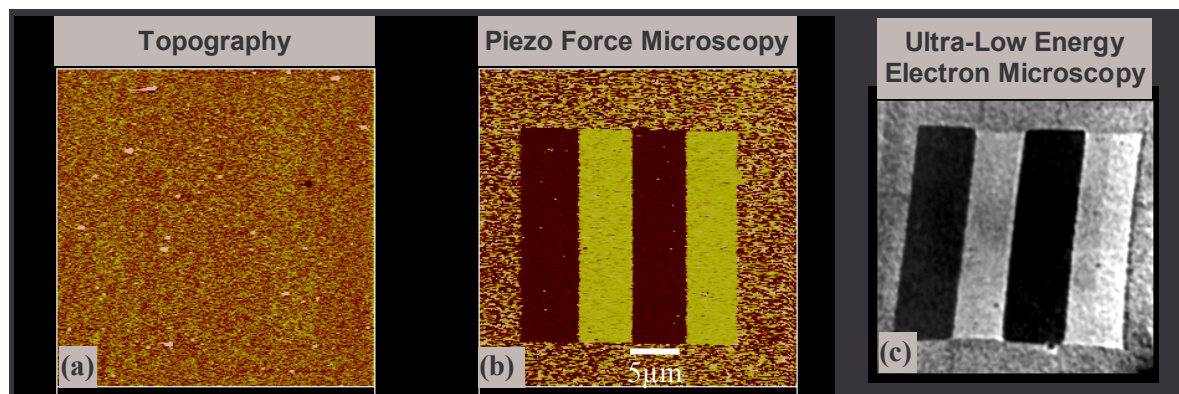


**Figure:** (a) Atomic force microscopy image showing the topography of the system after writing up/down – polarized ferroelectric domains in a multiferroic thin film; (b) Piezoelectric force microscopy image showing ferroelectric domains; (c) the corresponding low energy electron microscopy image



## Energy filtered imaging of photoemission threshold, core level and valence band of highly p and n doped pattern silicon

N. Barrett<sup>1</sup>, L.-F. Zagonel<sup>1</sup>, O. Renault<sup>2</sup>, A. Bailly<sup>2</sup>

<sup>1</sup> CEA DSM/IRAMIS/SPCSI, CEA Saclay, 91191 Gif sur Yvette, France

<sup>2</sup> CEA LETI Minatec, 17 rue des Martyrs, 38054 Grenoble cedex 9, France

Email: nick.barrett@cea.fr

Accurate description of spatial variations in the energy levels of patterned semiconductor substrates on the micron and sub-micron scale as a function of local doping is an important technological challenge for the microelectronics industry.

Spatially resolved spectromicroscopy can provide an invaluable contribution thanks to the relatively non-destructive, quantitative analysis. However, interpretation of the contrast mechanisms in PEEM is still open to debate. Surface states, doping levels [1], the oxide layer [2] and hot electron absorption near the Fermi level [3] can all contribute to observed contrast.

We present results on highly doped n and p type patterns, corresponding to source drain configurations on, respectively, p and n type silicon substrates. Using synchrotron radiation and aberration corrected energy filtering we have obtained spectroscopic image series at threshold, at the Si 2p core level and across the valence band. For the first time we observe clear contrast in the valence band.

Threshold imaging using a 4.9 eV laboratory source both confirmed previous non energy filtered studies [3] and also sheds light on the role of both the photon band width in the imaging contrast and residual surface carbon contamination under synchrotron radiation.

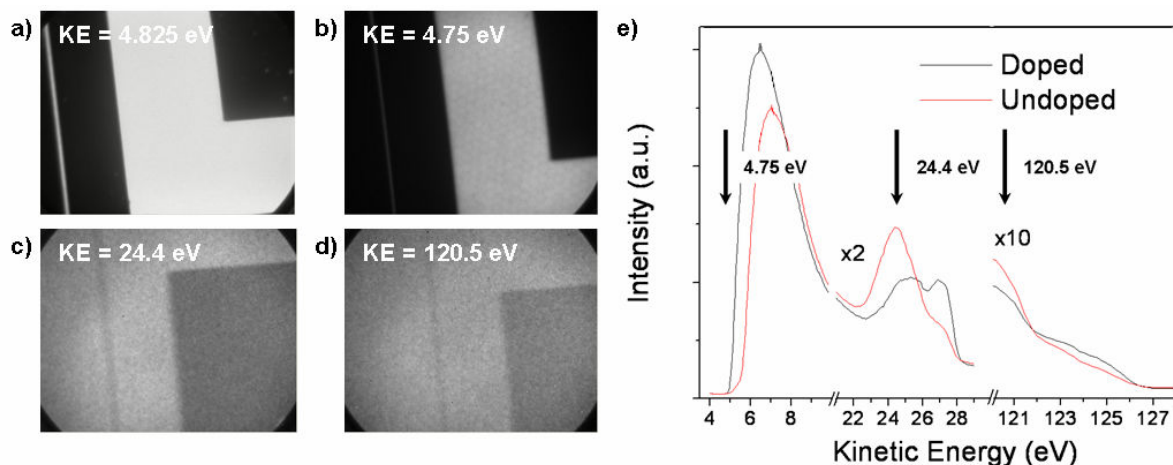


**Figure.** Energy filtered images for n-type patterns ( $10^{20} \text{ cm}^{-3}$ ) on the p type substrate ( $10^{17} \text{ cm}^{-3}$ ): a) at threshold using  $h\nu = 4.9 \text{ eV}$ ; b) at threshold, c) Si 2p and d) at the O 2p valence band edge using 130 eV synchrotron radiation; e) Photoemission spectrum extracted from the n-type doped pattern and p-type doped substrate.

### References

- [1] V.W. Ballarotto, K. Siegrist, R.J. Phaneuf, E.D. Williams *J. Appl. Phys.* **91** 469 (2002)
- [2] H. Fukidome, K. Tanaka, M. Yoshimura, K. Ueda, F.-Z. Guo, T. Kinoshita, K. Kobayashi *Surf. Sci.* **601** 4675 (2007)
- [3] L. Frank, I. Mullerova, D.A. Valdaitsev, A. Gloskovskii, S.A. Nepijko, H.-J. Elmers, G. Schönhense *J. Appl. Phys.* **100** 093712 (2006)

## LEEM Observation of Surfaces Using a Beam of Energetic Self-Ions

Wacek Swiech<sup>1</sup>, Mahesh Rajappan<sup>1,2</sup>, Michal Ondrejcek<sup>1,2</sup>, Ernie Sammann<sup>1</sup>,  
Steve Burdin<sup>1</sup>, Ivan Petrov<sup>1</sup> and C. Peter Flynn<sup>1,2</sup>

<sup>1</sup>Materials Research Laboratory and <sup>2</sup>Department of Physics  
University of Illinois at Urbana-Champaign, Urbana, IL 61801, U.S.A.

Email: wswiech@uiuc.edu

The MRL's LEEM instrument has recently been modified to incorporate a variable-energy source of negative ions created by cesium sputtering (SNICS). This allows the behavior of surface structures such as step edges to be observed at video rates *in-situ* during the actual ion irradiation. Ion beam irradiation can exert considerable influence on the structure and behavior of materials at the nanoscale. As a research tool, ion beams provide an opportunity to perturb the equilibrium of the surface, affording access to metastable states and dynamics not easily attained by other means.

Two general categories of applications will be sketched [1-4]. Experiments that permit quantitative determination of important physical quantities include: surface mass diffusion over an extended temperature range; determining the critical chemical potential at which island nucleation occurs; observation and explanation of the universal evolution by which adatom and advacancy islands both grow and shrink by beam-driven processes; and the study of sublimation (regarded as negative ion beam intensity). Further experiments described include beam-assisted synthesis first of large pans and mesas for isolating surface experiments (e.g. nucleation) from the surrounding crystal. Moreover synthesis of Fourier waves on steps, for studies of diffusive relaxation. Operation of exotic structures including Bardeen-Herring sources and Franck growth spirals deformed by crystal anisotropy are also described.

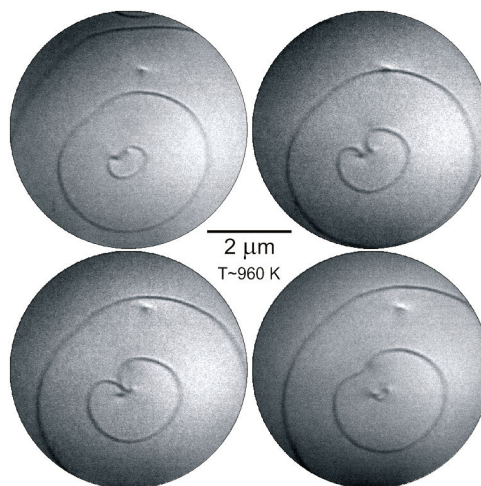


**Figure.** Evolution of a Bardeen-Herring source on a pan at T~960 K. The Burgers vector points out of the surface plane and creates a step edge terminated by two screw dislocations of the opposite sign.

### References

- [1] Swiech W, Rajappan M, Ondrejcek M, Sammann E, Burdin S, Petrov I and Flynn C P *Ultramicroscopy* 2008, in print (doi: 10.1016/j.ultramic.2007.10.005)
- [2] Flynn C P, Swiech W, Ondrejcek M and Rajappan M 2008 *Phys. Rev.* B77, 045406
- [3] Rajappan M, Swiech W, Ondrejcek M and Flynn C P 2007 *Phil. Mag.* 87, 4501
- [4] Rajappan M, Swiech W, Ondrejcek M and Flynn C P 2007 *J. Phys.: Cond. Matter* 19, 226006

## Imaging Oxide-Covered Doped Silicon Structures Using Low-Energy Electron Microscopy

M. L. Anderson<sup>1</sup>, C. Y. Nakakura,<sup>1</sup> and G. L. Kellogg<sup>1</sup>

<sup>1</sup>Sandia National Laboratories\*, Albuquerque, NM 87185 US

Email: mlande@sandia.gov

Owing to the increasing complexity of integrated circuits, quantitative 2-D imaging techniques that analyze the dopant characteristics of state-of-the-art devices have become a necessity. The sensitivity of LEEM to surface morphology, work function differences and surface charge variations makes it an ideal instrument for studying devices. In this talk, we present recent progress towards imaging doped silicon devices using LEEM. Diode test structures were fabricated with *n/p* junctions buried under thermally grown oxides. Significant *n/p* contrast was observed for the buried structures at electron energies just above the mirror mode (Fig. 1a). To determine the origin of the contrast, we measured current-voltage (IV) curves over the mirror-to-LEEM electron energy range. The measurement is complicated by the fact that the oxide charges when exposed to the electron beam. Direct evidence for charging is shown in Fig. 1, in which the sample is translated under the imaging beam. The freshly exposed region (Fig. 1b) is momentarily dark in the *p*-type region, and then proceeds to get bright as a function of time (Fig. 1c). To overcome the effects of charging, we developed a method to measure “pre-charging” IV curves. The method was applied to a series of samples with varying oxide thickness (~25 to ~500 Å). The resulting IV curves show that onset of charge flow to the sample depends on doping type *and* oxide thickness indicating that *both* contribute to the observed contrast. The dependence of the IV curves on oxide thickness suggests that the oxide is charged even before beam exposure and that LEEM measurements are potentially useful to characterize the spatial distribution of charge traps in thermal oxides.

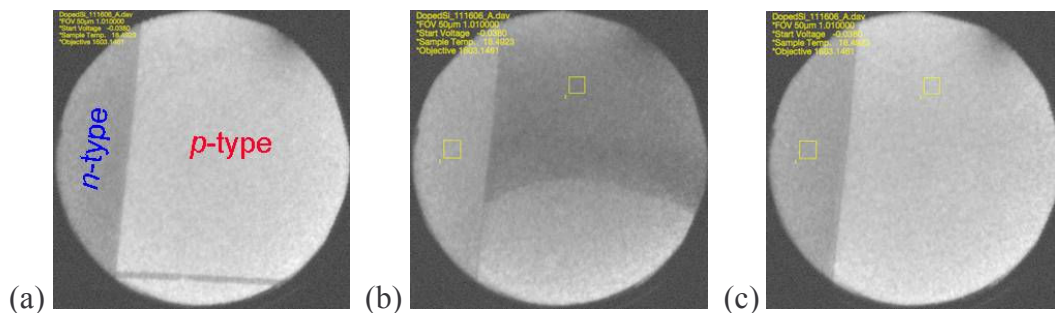


**Figure.** LEEM images showing oxide charging. Start voltage = 0 V, field of view = 50  $\mu\text{m}$ .

\*Sandia is a multiprogram laboratory operated by Sandia Corporation, a Lockheed Martin Company for the USDOE’s NNSA under contract DE-AC04-94AL85000.

## REM, LODREM and LEEM comparison for surface studies

J.J. Métois<sup>1</sup>, B. Ranguelov<sup>1,2</sup>, P. Müller<sup>1</sup>, F. Leroy<sup>1</sup>

<sup>1</sup>Aix-Marseille Université- Centre Interdisciplinaire de Nano-sciences de Marseille,  
CINaM-CNRS, Campus de Luminy, case 913, 13288 Marseille cedex, France

<sup>2</sup>Institute of Physical Chemistry – Bulgarian Academy of Sciences, “Acad. G. Bonchev” Str., bl. 11,  
1113- Sofia, Bulgaria

Email: muller@cinam.univ-mrs.fr

Reflection Electron Microscopy (REM) and Low Energy Electron Microscopy (LEEM) are widely used to study surface dynamic processes. One of the main disadvantages of REM is that because of the glancing incident angle of the electron beam, REM images are severely foreshortened in one direction by a factor varying between 1/40 and 1/70. A correction of the images is thus necessary to get an undistorted view of the surface morphology. However, because of the limitation due to the pixel size, a numerical correction is not sufficient.

We will show that a simple geometrical modification of the REM column, based on a controlled tilt of the screen, enables a correction of the distortion (Figure). We will use the acronym LODREM for such Low Distortion Reflection Electron Microscopy [1]. Our goal in this contribution is to compare LODREM and LEEM capabilities. For this purpose we will essentially compare REM, LODREM and LEEM images of the same surfaces.

At last we have studied by LODREM, the homoepitaxial growth and evaporation of Si(111) surfaces *via* spirals, in perfectly controlled thermodynamics conditions [2]. It is found that the dynamics of these spirals deviates from the usual Burton Cabrera Franck (BCF) scaling law, in agreement with more recent models in which non local dynamic effects are taken into account and considering that the attachment kinetics of the adatoms at kink sites is the limiting process of step flow (or retraction).

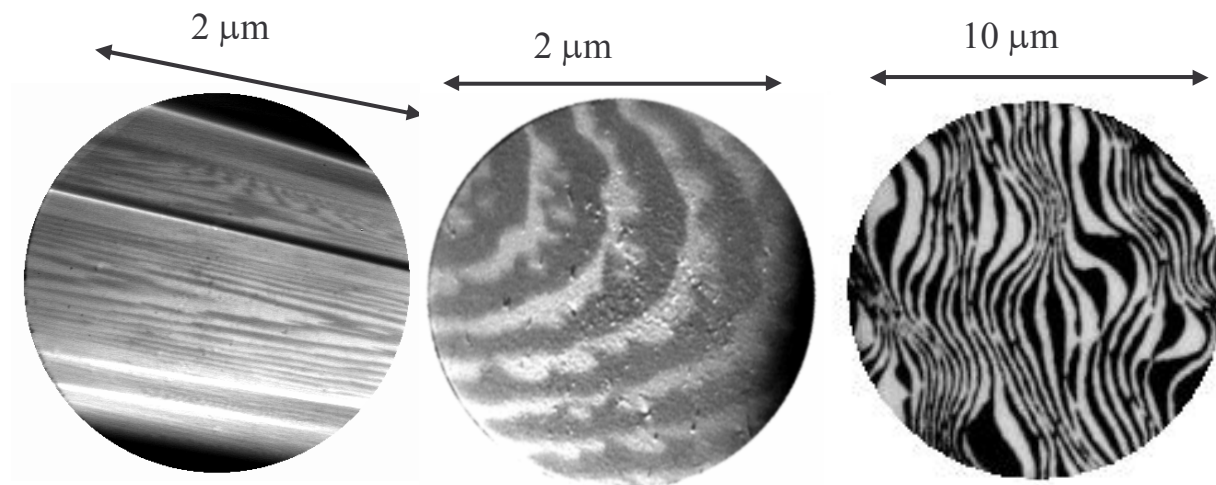


**Figure.** Si(001) Surface. (a) REM, (b) LODREM and (c) LEEM [3] images

### References

- [1] P. Muller and J.-J. Métois, Surface Science 599, 2005, p187-195.
- [2] B. Ranguelov, J.-J. Métois and P. Müller, Surface Science, 600, 2006, p4848-4854
- [3] R.M. Tromp, IBM J. Res. Dev., 44, 2000, p503